DOI: 10.1002/cmdc.200700270

Computer-Aided Design and Synthesis of Nonpeptidic Plasmepsin II and IV Inhibitors

Torsten Luksch,[a] Nan-Si Chan,[a] Sascha Brass,[a] Christoph A. Sotriffer,[b] Gerhard Klebe,[a] and Wibke E. Diederich*[a]

Plasmepsins (Plm) II (EC number: 3.4.23.39) and IV (EC number: 3.4.23.B14) are aspartic proteases present in the food vacuole of the malaria parasite Plasmodium falciparum *and are involved in host hemoglobin degradation. Based on our established efficient synthetic sequence, a series of inhibitors for Plm II and IV has been synthesized bearing a 2,3,4,7-tetrahydro-1*H*-azepine scaffold as the core structural element. During the computational design cycle, thorough investigations were carried out in order to find a reasonable theoretical binding mode for Plm II and IV. The conformation of Plm II in the crystal structure (PDB code: 1LF2) provides a good starting geometry for our virtual screening approach. In contrast, the only available co-crystal structure for Plm IV of* P. falciparum *(PDB code: 1LS5) appears inappropriate for inhibitor design. Therefore, a homology model was constructed based on the Plm II 1LF2 structure. A combinatorial docking run using FlexX*[c] *suggested compounds which, after synthesis, turned out to exhibit affinities in the sub-micromolar range. The observed structure–activity relationships of the synthesized compounds confirm the assumed binding mode for Plm II and IV. The best-binding inhibitors designed for Plm II and IV are devoid of any inhibitory potency against human cathepsin D (EC number: 3.4.23.5).*

Introduction

The protozoan disease malaria is still one of the major inexorable infections worldwide, and it is especially widespread throughout tropical regions. It is caused by parasites of the genus *Plasmodium* (*P. falciparum*, *P. vivax*, *P. malariae*, and *P. ovale*) and transmitted by female *Anopheles* mosquitoes. The World Health Organization (WHO) estimates that approximately 350 to 500 million people are infected annually.[1] Infections by *P. falciparum*, the most severe form of malaria, are responsible for or at least contribute to more than a million deaths per year. Children below the age of five are particularly affected.[1] The continuously increasing resistance of the vector toward insecticides as well as the emergence of multidrug-resistant parasites greatly necessitates the development of new anti-infective substances that have either a novel binding mode or a new mechanism of action, which is pivotal to combat this life-threatening disease.

During its life cycle, *P. falciparum* degrades the hemoglobin of the host cell to cover the energy and nutritional demands for its own growth and maturation. In this metabolic pathway, the following proteolytic enzymes are hitherto known to be involved: aspartic proteases (plasmepsin (Plm) I,[2,3] II,[4,5] IV,[6] and the closely related histoaspartic protease (HAP)[6,7]), cysteine proteases (falcipain 1,[8,9] 2,[10,11] and 3[12]), a metalloprotease (falcilysin),[13] and the recently discovered dipeptidyl aminopeptidase 1 (DPAP1).[14] The degradation process appears to follow an ordered pathway.[4,13] Although the precise sequence of events, particularly whether a plasmepsin or a falcipain catalyzes the initial degradation step,[4,15] is still under debate, it has been shown that malaria parasites, both in culture and in animal models, are eradicated by Plm inhibitors, thus providing a proof-of-concept that these proteases are viable drug targets.[2,16–18] Initial experiments with *P. falciparum* Plm knockout clones indicated the necessity of simultaneously inhibiting several of the food vacuole Plms in order to effectively tackle the parasite.[19–21] Recently, Bonilla et al. demonstrated that the growth of the intraerythrocytic-stage parasite is attenuated only in mutants that lack all four digestive vacuole plasmepsins.[22] The design of compounds that are able to inhibit all food vacuole Plms in parallel seems to be necessary not only for the efficient eradication of the parasite, but also to impede the development of parasite resistance. In particular, Plm IV plays a crucial role, as it is the only Plm of *P. falciparum* with orthologs in the other *Plasmodium* species that infect humans and therefore opens a way to affect all the *Plasmodium* parasites with one inhibitor.[23]

Most inhibitors synthesized so far against Plm II are peptidomimetic transition-state analogues[24] that address the two aspartates of the active site by a hydroxy or hydroxy-like moiety, thereby replacing the native substrate. These peptidomimetic inhibitors are highly active but often suffer from low bioavailability and are difficult to synthesize. Several years ago, Oefner et al. identified by high-throughput screening nonpeptidic inhibitors for renin,[25] a structurally related aspartic protease

[a] *Dr. T. Luksch,[+] N.-S. Chan,[+] Dr. S. Brass, Prof. Dr. G. Klebe, Dr. W. E. Diederich*
Institut für Pharmazeutische Chemie, Philipps-Universität Marburg
Marbacher Weg 6, 35032 Marburg (Germany)
Fax: (+49) 6421-28-26254
E-mail: wibke.diederich@staff.uni-marburg.de

[b] *Prof. Dr. C. A. Sotriffer*
Institut für Pharmazie und Lebensmittelchemie, Universität Würzburg
Am Hubland, 97074 Würzburg (Germany)

[+] *These authors contributed equally to this work.*

with 35% sequence identity to Plm II. These inhibitors all feature a piperidine scaffold that addresses the two catalytic aspartates through its basic and most likely protonated secondary endocyclic amino functionality. Interestingly, some of these inhibitors also show moderate activity against Plm I and II. Recently, substituted pyrrolidines have been described as micromolar inhibitors of the aspartic protease HIV-1.[26] Diederich and co-workers identified a 7-azabicyclo[2.2.1]heptane scaffold as an adequate core structure for the development of Plm II and IV inhibitors.[27,28] These results prompted us to investigate in greater detail the suitability of azacycles bearing a basic amino functionality as core element for the design and synthesis of Plm inhibitors.

So far, 15 *P. falciparum* Plm II–inhibitor complex structures have been deposited in the Protein Data Bank (PDB); 14 of these can be classified in three groups exhibiting different ligand binding modes: 1) Eight complexes contain either pepstatin A or a closely related pepstatin A analogue as inhibitor. As transition-state analogues they exhibit an almost identical ligand binding mode (PDB codes: 1SME,[29] 1ME6, 1XDH, 1XE5, 1XE6, 1W6I, 1W6H, and 1M43) (Figure 1 a). The flap lid shared by all aspartic proteases folds on the bound inhibitor and puts the binding pocket in the closed state. 2) The second group comprises three complexes (1LF2, 1LEE, and 1LF3)[30,31] in which the binding pocket is in a partially open conformation (Figure 1 b). 3) In the third group, a new specificity pocket, the so-called flap pocket, is unlocked and addressed by the inhibitors (2BJU ($K_i = 34$ nM),[32] 2IGY,[18] and 2IGX[18]) (Figure 1 c).

The crystallographically indicated adaptivity of the protein is further confirmed by molecular dynamics (MD) simulations.[33–36] They suggest that Plm II and most likely Plm I and IV are highly flexible proteins that adopt additional conformations not yet characterized, but which could possibly be targeted by inhibitors.[37]

Because only three distinct binding modes have been discovered so far, and due to the fact that the target protein has been treated as rigid in most in silico studies, the application of automated docking procedures appears rather limited. Moreover, there are some reported cases in which docking failed to predict reasonable binding modes based on previously determined crystal structures.[35,36,38] The situation appears even worse for *P. falciparum* Plm IV, as for this enzyme only a single co-crystal structure in complex with pepstatin A is available (PDB code: 1LS5). For Plm I, only one homology model has been described so far.[29] An in-depth literature search indicates that a possible explanation for the rather poorly described structural properties of these enzymes might originate from difficulties in growing crystals that diffract sufficiently well for structure determination of complexes with inhibitors that do not adopt a pepstatin-like binding mode. However, as our goal is the design and synthesis of promiscuous inhibitors that address Plm II and IV equally well, we planned an azacyclic scaffold as suitable geometry for docking into one of the currently available crystal structures.

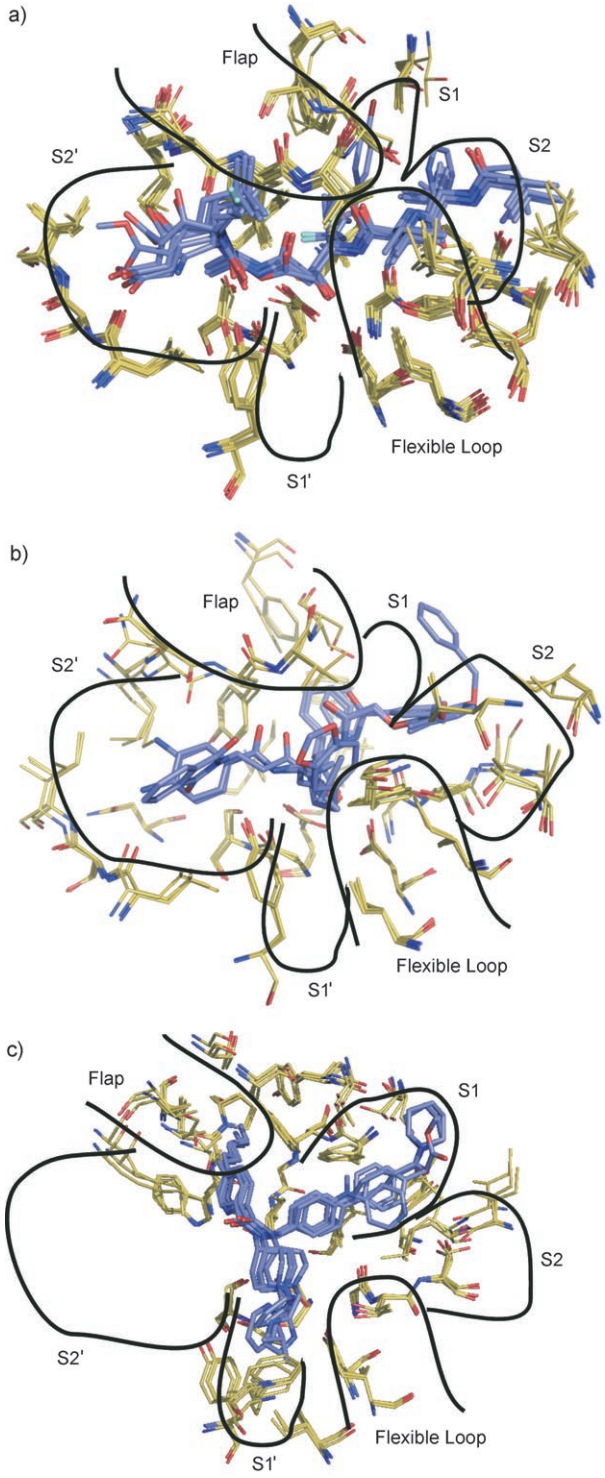

Figure 1. Superposition of a) all pepstatin and pepstatin-like ligands from Plm II crystal structures, b) all crystal structure ligands that generate a more open binding pocket, and c) all inhibitors found in crystal structures that address a new specificity pocket. All amino acids up to 6 Å away from the ligands are shown in stick representation. Ligands are shown in blue, color-coded by atom type, amino acids in yellow, color-coded by atom type. Image created using PyMol 0.99.[59]

Results and Discussion

In silico evaluation of the core structure

Preliminary modeling studies suggested that a 2,3,4,7-tetrahydro-1*H*-azepine scaffold could provide a promising starting point for the design of putative Plm inhibitors. As depicted in Figure 2, the azacycle could address the two aspartates of the catalytic dyad by its basic nitrogen atom.

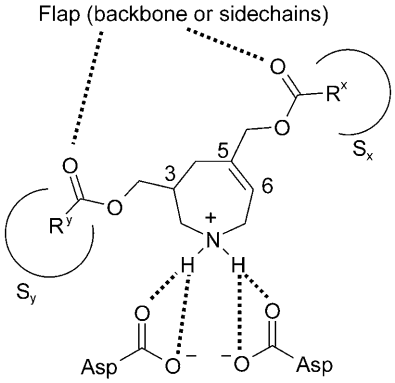

Figure 2. 3,5-Bis-carbonyloxymethyl-substituted azepine template and its putative hydrogen-bond network within the active site of Plm.

Equipped with appropriate linker groups at positions 3 and 5, the introduction of well-tailored substituents to explore and specifically address the various substrate recognition pockets is easily carried out. As a starting point we selected (*rac*)-3,5-bis-hydroxymethyl-2,3,4,7-tetrahydro-1*H*-azepine. The primary hydroxy functionalities on this core structure can readily be esterified by using standard coupling reactions.

The carbonyl oxygen atoms of both ester groups are thought to be well placed to establish hydrogen bonds to the flap region. Following our synthetic strategy, the azepine derivatives are obtained as racemic mixtures resulting from the evolving stereocenter at position 3 of the ring system.[39] To obtain further insight into a putative binding mode, the *R* and the *S* enantiomers were docked with FlexX.[40] The protein conformers found in the crystal structures 1SME (pepstatin-like), 2BJU (flap pocket), and 1LF2 (opened binding pocket) were used as reference geometries (Table 1). In all cases, the *R* enantiomer had better scores in terms of the FlexX scoring function. Furthermore, in the conformer displayed in the crystal structure 1LF2, the *R* enantiomer received the best scoring relative to the other two Plm conformers.

Closer investigation of the crystal structure 1LF2 with its bound parent inhibitor RS367 revealed that the hydroxy group of the hydroxypropylamine isostere establishes hydrogen bonds to the catalytic dyad (Figure 3a). In addition, hydrogen bonds are formed to the flap residues V78 and S79.

Comparison of a docking pose of our azepine derivative (Figure 3b) with the crystal structure of the RS367 ligand (K_i = 30 nM) suggests a similar hydrogen-bond pattern; in our case, the quaternary amino group of the azepine moiety interacts

Table 1. Scores of the FlexX^c scoring function.[a]

PDB code	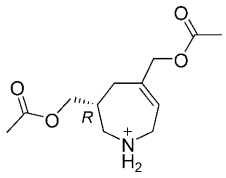	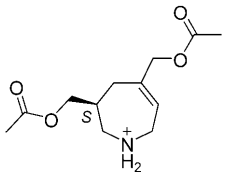
1SME	−18.5	−17.8
2BJU	−16.1	−14.2
1LF2	−24.8	−18.2

[a] Scores of the FlexX^c scoring function generated for the *R* (left) and *S* enantiomer (right) as docked into three different Plm II crystal structure geometries (1SME, 2BJU, and 1LF2).

through charge-assisted hydrogen bonds with the two aspartates of the catalytic dyad. The carbonyl oxygen atom of the ester function at position 3 addresses the backbone NH group of V78 in the flap, whereas the ester carbonyl oxygen at position 5 forms a hydrogen bond to the hydroxy group of S79 in the flap region. In this docking solution, the two terminal methyl groups are oriented toward the S1 and S2′ pockets. Considering the placement of the methoxy bond vectors, a variety of different ester substituents can be added to properly address the corresponding subpockets.

With respect to the ring structure of the azepine moiety, the boat conformation generated by Corina[41] and used for docking with FlexX appears to be an acceptable low-energy conformation. Support for this assumption comes from the observation that the 2,3,4,7-tetrahydro-1*H*-azepine scaffold can indeed show a boat conformation in crystal structures (see entry CCDC 260740[42] in the Cambridge Structural Database[43]). Furthermore, conformational NMR studies on cycloheptene ring systems have provided examples in which the boat conformation is virtually as favored as the chair conformation.[44,45]

Docking starting geometry for Plm IV

For Plm IV of *P. falciparum*, only a co-crystal structure with pepstatin A is available.[31] The binding mode of the inhibitor in this complex is very similar to that of pepstatin A in Plm II, which also results in a binding site conformer with closed flap lids. Based on the docking results of our core structure with the three distinct protein conformations that suggest preferred binding to the open conformer of Plm II, we propose that in the case of Plm IV as well a more open protein conformation is required to accommodate our azepine derivatives. Plm IV exhibits high sequence identity (69%) to Plm II. In the whole binding pocket, 24 out of 34 residues are conserved considering all residues up to 6 Å distant from the ligand RS367. Thus, a reasonable homology model of Plm IV could be generated in the more open conformation based on the coordinates of the complex structure of Plm II (1LF2) as template. Gutiérrez-de-Terán et al. also generated a Plm IV homology model based on Plm II structures.[46]

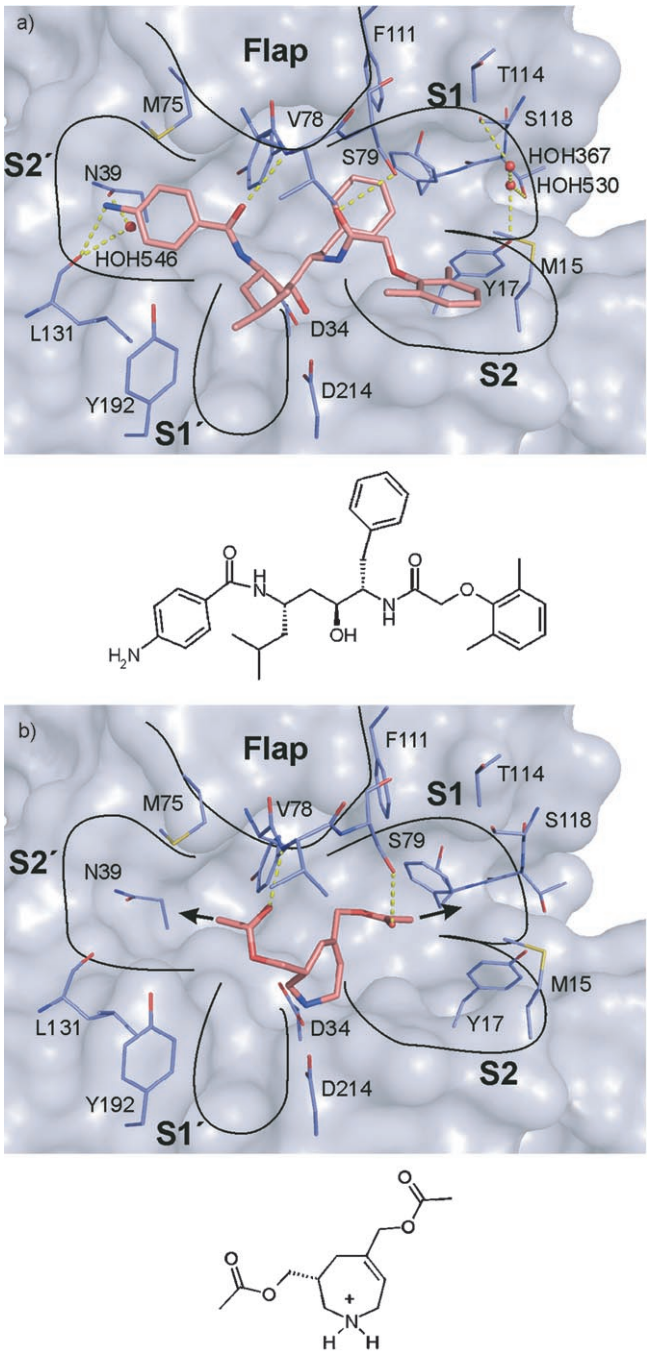

Figure 3. a) Crystal structure 1LF2 (surface and stick representation in blue, amino acids color-coded by atom type) in complex with RS367 (stick representation in salmon, color-coded by atom type). Hydrogen bonds to the flap amino acids V78 and S79 are formed. The catalytic dyad (D34 and D214) is addressed by a hydroxy group. The S1, S2, S1′, and S2′ pockets are occupied by the inhibitor. b) Docking solution of the azepine core structure (*R* enantiomer, salmon, color-coded by atom type) in 1LF2 (blue). Hydrogen bonds to the flap and to the catalytic dyad are formed. The two substituents point toward the S1 and S2′ pockets. Image created using PyMol 0.99.[59]

Optimization of the P1 and P2′ residues

Docking of the parent core structure suggested preferred binding of the *R* enantiomer of our azepine to the open protein conformer, which was therefore considered for the further optimization process. Putative substitution vectors (R_x, R_y) point toward the S2′ and S1 pockets (Figures 2 and 3b). In the following, these pockets were thoroughly analyzed to identify putative substituents to optimally address both specificity pockets. To gather ideas of potential occupants for these pockets, we first performed a database search using Cavbase to retrieve similar subpockets present in other crystal structures.[47,48] Cavbase is a method to describe and compare protein binding pockets in terms of shape and exposed physicochemical properties. As a matter of fact, most pockets that exhibit a pronounced physicochemical similarity to the Plm II recognition pockets also turned out to be members of the class of aspartic proteases. The molecular portions of ligands found to occupy similar subpockets were extracted and analyzed for their suitability as building blocks for the synthesis of putative inhibitors. In approximately one third of all retrieved pockets that show similarity to the Plm II S1 pocket, a phenyl moiety was consistently found (31 out of 100 similar pockets). A similar search performed for the S2′ pocket was less conclusive, and a broad spectrum of structurally diverse molecular building blocks was suggested. This indicates that the specificity of this pocket is less pronounced for a single preferred occupant. As we planned to perform our design in a stepwise fashion, we decided to use a phenyl moiety initially as most suitable occupant to address the Plm II S1 pocket. The S2′ pocket, as indicated by our Cavbase search, is less discriminative for a particular substituent.

We therefore decided to perform a rather exhaustive screen for putative occupants using combinatorial docking with FlexX[c]. From a synthetic point of view, we intended to apply ester bond formation. As a consequence, we retrieved a diverse set of 2083 carboxylic acids from the Sigma–Aldrich catalogue. All considered acid fragments had a molecular weight below 250 Da. Based on the benzoyloxymethylazepine core structure, a library of 2083 esters was generated on the computer (Scheme 1).

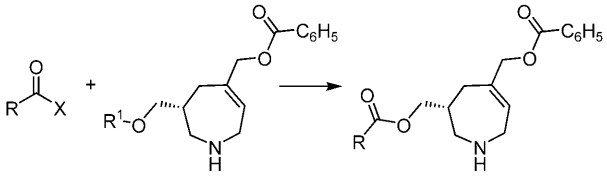

Scheme 1. A library of 2083 esters was generated by linking the core with the fragments.

Subsequent to docking, a visual inspection of the 100 best-scored candidates was performed. The parent crystal structure 1LF2 with RS367 shows three water molecules that mediate interactions to the bound ligand or to the protein. These water molecules present in the S1 and S2′ pockets possess rather low *B* factors. Similarly placed water molecules could potentially influence the binding modes of our docked library entries. HOH546 with a *B* factor below 10 Å^2, located in the S2′ pocket, establishes hydrogen bonds to the N39 side chain and to the carbonyl oxygen atom of L131. HOH367 (*B* factor = 24 Å^2) and

HOH530 (*B* factor = 19 Å^2) both occupy the S1 pocket and mediate a hydrogen bonding network between S118, Y17, and T119 (Figure 3a). As these water molecules were not considered during our initial combinatorial docking run, we added them in an additional energy-minimization step in order to optimize the ligand geometries of the best-scored candidate ligands in the presence of these water molecules. During minimization with the Moloc MAB force field,[49] the protein and water atoms were kept rigid, whereas the ligand was assigned to full flexibility.

Analysis of the docked ligands

In almost all docking solutions, the protonated amino functionality of the azepine core interacts with the two aspartates of the catalytic dyad as suggested by our initial docking runs (Figure 3b). The ester functionality in position 5 forms a hydrogen bond to the flap residue S79. Its phenyl ring occupies the predominantly hydrophobic S1 pocket (Figure 3b) composed by M15, I32, F111, and F120. The carbonyl oxygen atom of the ester functionality at position 3 forms a hydrogen bond to the flap backbone NH group of V78. As expected, in almost all docking solutions the attached R groups of the 2083 library members occupy the S2′ pocket. Among the best-scored solutions, aromatic ring moieties bearing hydroxy or amino substituents at various ring positions were preferentially detected.

Similar combinatorial docking followed by a subsequent energy-minimization step was performed for the Plm IV homology model using the same library of candidate ligands as for Plm II. The docking results showed very similar binding poses and preferences; the phenyl moiety at position 5 fills the S1 pocket in a similar fashion. For the P2′ substituent, aromatic ring systems equipped with hydroxy or amino groups at various ring positions are also highly scored for this isozyme.

Synthesis and biological testing of the first design series

Based on the design hypothesis derived from our first cycle, and also considering the synthetic feasibility of the proposed molecules, inhibitors (*rac*)-**1**, (*rac*)-**2**, and (*rac*)-**3** were prepared according to the synthesis scheme described below (Scheme 2 and reference [39]). The compounds were tested for activity against Plm II, Plm IV, and the related human aspartic protease cathepsin D (Table 2). Compound (*rac*)-**1** showed a K_i value of 4.7 μM for Plm II and 7.2 μM for Plm IV. In agreement with our modeling results, the importance of the amino group is dem-

Table 2. Experimental inhibitory activities of the compounds studied.[a]

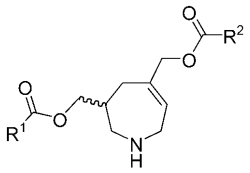

Compd	R^1	R^2	K_i [μM] Plm II	Plm IV	Cat D
1	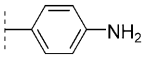		4.7	7.2	260
2			303	211	⩾320
3	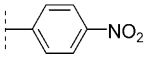		28.8	38.6	348
4	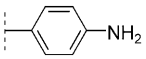	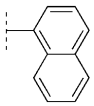	1.0	1.5	262
5	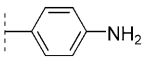	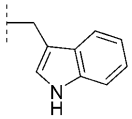	2.4	15.9	>100
6	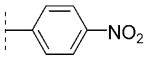	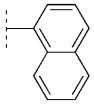	1.3	3.9	51
7	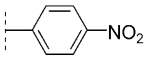	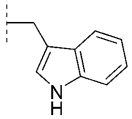	4.7	43.4	>100
8		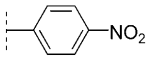	28.8	29.0	285
9		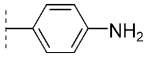	7.6	9.9	255
10	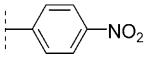	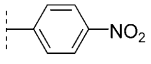	10.9	22.1	321
11	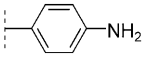	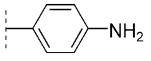	0.8	3.2	142
12	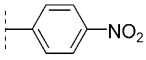	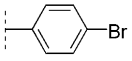	49.0	68.8	178
13	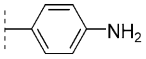	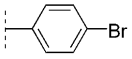	0.4	5.7	165

[a] Compound (*rac*)-**11** was obtained as its trihydrochloride salt, the other compounds as their monohydrochloride salts.

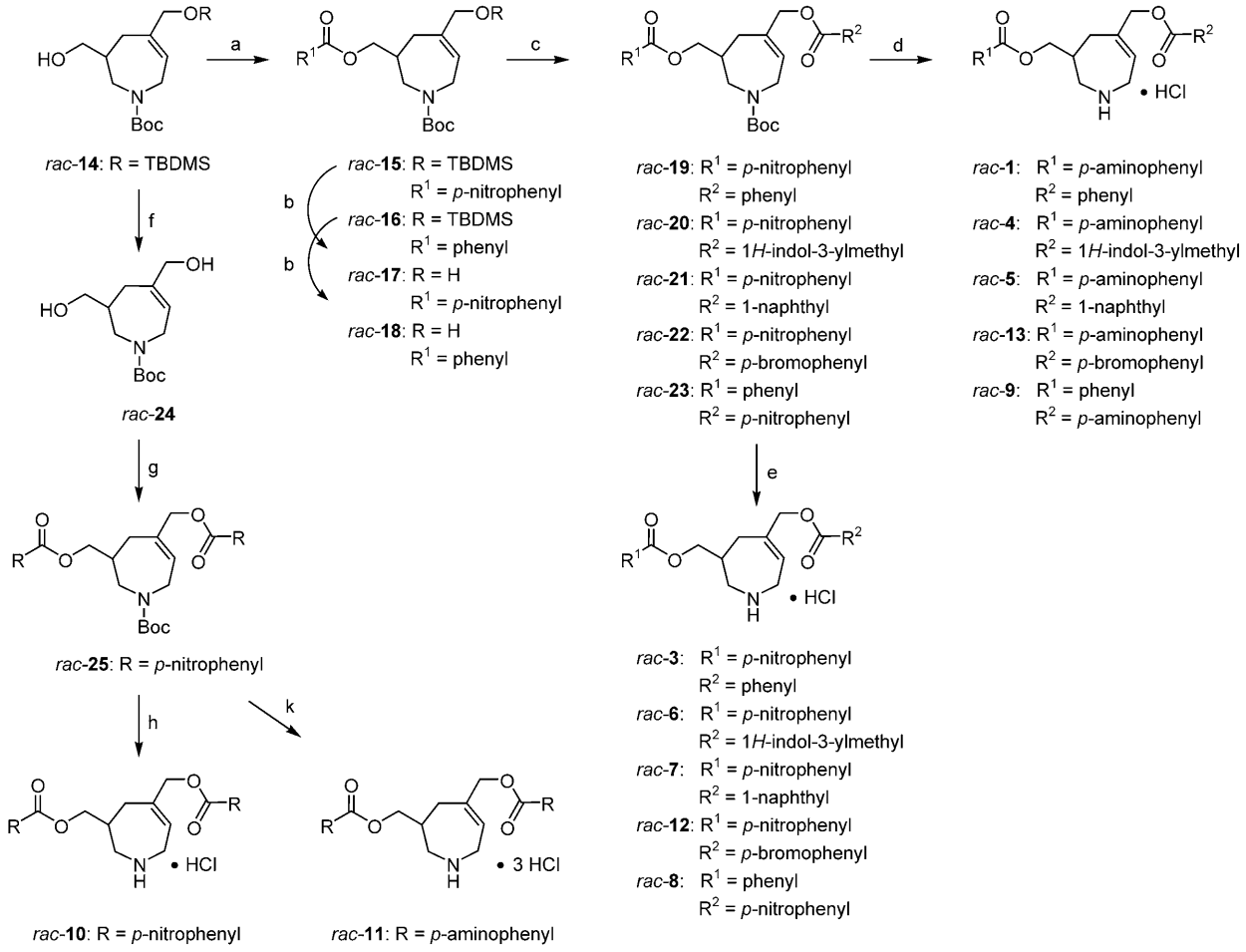

Scheme 2. Synthetic pathway toward inhibitors (*rac*)-**1**, (*rac*)-**3** to (*rac*)-**13**. Reagents and conditions: a) for (*rac*)-**15**: *p*-nitrobenzoic acid, THF/CH_2Cl_2 1:1, DIC, DMAP, 12 h, 71%; for (*rac*)-**16**: benzoyl chloride, CH_2Cl_2, TEA, DMAP, 18 h, 72%; b) 1% $HCl_{(aq)}$ in THF, room temperature; for (*rac*)-**17**: 30 min, 77%; for (*rac*)-**18**: 30 min, 90%; c) for (*rac*)-**19**: benzoyl chloride, CH_2Cl_2, TEA, DMAP, 16 h, 87%; for (*rac*)-**20**: 3-indole acetic acid, THF/CH_2Cl_2 1:1, DIC, DMAP, 14 h, 84%; for (*rac*)-**21**: 1-naphthoic acid, THF/CH_2Cl_2 1:1, DIC, DMAP, 12 h, 44%; for (*rac*)-**22**: *p*-bromobenzoic acid, THF/CH_2Cl_2 1:1, DIC, DMAP, 14 h, 58%; for (*rac*)-**23**: *p*-nitrobenzoic acid, THF/CH_2Cl_2 1:1, DIC, DMAP, 18 h, 65%; d) 1) $SnCl_2{\cdot}2H_2O$ in EtOAc, 80 °C, 3 h, 2) 2 M HCl in Et_2O, room temperature, 24 h; for (*rac*)-**1**: 48%; for (*rac*)-**4**: 52%; for (*rac*)-**5**: 73%; for (*rac*)-**13**: 47%; for (*rac*)-**9**: 70%; e) 2 M HCl in Et_2O, room temperature, 24 h; for (*rac*)-**3**: 91%; for (*rac*)-**6**: 85%; for (*rac*)-**7**: 91%; for (*rac*)-**12**: 94%; for (*rac*)-**8**: 88%; f) ref. [39]; g) *p*-nitrobenzoic acid, THF/CH_2Cl_2 1:1, DIC, DMAP, 13 h, 69%; h) 2 M HCl in Et_2O, room temperature, 24 h, 96%; k) 1) $SnCl_2{\cdot}2H_2O$ in EtOAc, 80 °C, 3 h, 2) 2 M HCl in Et_2O, room temperature, 24 h, 59%. DIC = 1,3-diisopropylcarbodiimide, DMAP = 4-dimethylaminopyridine, TEA = triethylamine.

onstrated by the 60-fold difference in affinity between (*rac*)-**1** and (*rac*)-**2**. The latter lacks a similar H-bond donor group. In addition, the synthetic precursor of (*rac*)-**1**, compound (*rac*)-**3** bearing a *p*-nitrobenzoyloxymethyl substituent at position 3 of the azepine ring, was tested for Plm inhibition. However, in contrast to our prediction from docking, its K_i values for Plm II and Plm IV are unexpectedly low (29.0 and 38.6 μM, respectively). This compound receives a scoring worse than the unsubstituted (*rac*)-**2**. Assuming a similar binding pose of (*rac*)-**3** relative to (*rac*)-**1** (Figure 5a) and (*rac*)-**2**, the *p*-nitrobenzoyloxymethyl moiety should experience repulsive interactions between its nitro group and the side chain amide oxygen atom of N39 in the S2′ pocket.

In the search for a possible explanation for this unexpected finding, MD simulations of the noncomplexed protein were performed. Along the trajectory, pronounced side chain movements of N39 in the S2′ pocket could be observed. In addition to the conformation found in the crystal structure, a further low-energy conformer seems to be significantly populated (Figure 4).

In this second conformation, the Nχ2 angle is rotated by 180°. Based on this alternative conformer, a reasonable binding geometry for (*rac*)-**3** can be suggested. The azepine moiety and the P1 substituent of (*rac*)-**3** both remain bound to the protein in a similar fashion. However, the *p*-nitro group of the P2′ substituent replaces HOH546 and forms a direct hydrogen bond to the terminal carboxamide NH group of the rotated N39 residue. This binding pose is in agreement with the enhanced binding affinity of the nitro derivative relative to the unsubstituted derivative (*rac*)-**2**.

A second design cycle was performed in which the substituent for the S1 pocket was optimized, keeping the previously detected P2′ substituent unchanged. Again, ester bond formation was envisaged for synthetic reasons. A similar combinato-

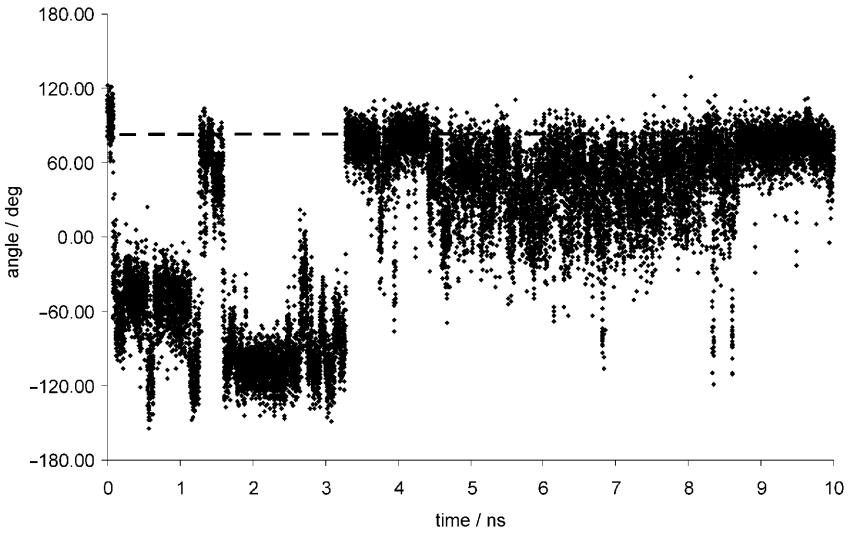

Figure 4. Fluctuation of the Nχ2 angle in Asn39 (N39) of Plm II observed in the MD simulation, with the respective value from the crystal structure shown as reference; see the Experimental Section for details.

rial docking run using FlexX[c] was carried out following a subsequent energy-minimization step.

An extended set of P1 substituents with either multiple rotatable bonds or peptidic character received high scoring for Plm II and Plm IV. To avoid these undesired solutions, we applied a filter and only allowed substituents without amide bonds and a limited number of rotatable bonds. Among the remaining most promising candidates, a 1*H*-indolyl-3-methyl substituent could be detected. It potentially forms a hydrogen bond to S218 (Figure 5 b). Sterically more demanding hydrophobic groups such as a naphthyl moiety followed on subsequent ranks. As a consequence (Scheme 2), the *p*-amino derivatives (*rac*)-**4** and (*rac*)-**5** were synthesized along with their nitro-substituted precursors (*rac*)-**6** and (*rac*)-**7**. Compared with the phenyl derivative (*rac*)-**1**, both the 3-indolyl acetic acid substituted inhibitor (*rac*)-**4** and the naphthyl derivative (*rac*)-**5** show improved binding toward Plm II. With respect to Plm IV, only the indolyl-type inhibitor (*rac*)-**4** achieves better binding. The naphthyl derivative (*rac*)-**5** drops slightly relative to the phenyl compound (*rac*)-**1**. For Plm II, both nitro derivatives (*rac*)-**6** and (*rac*)-**7** experience improved binding compared with (*rac*)-**3**. The same holds for the binding of (*rac*)-**6** to Plm IV, whereas (*rac*)-**7**, in agreement with the amino series, shows nearly unchanged affinity.

Based on these results we entered into a third design cycle. The modeled binding pose of (*R*)-**1** or (*R*)-**7** suggested the introduction of a polar substituent either at the *para* position of the phenyl ring or the 2-position of the naphthyl moiety in position 5 of the azepine core. Such substituents could possibly interact with the neighboring water molecules present in the crystal structure with RS367. To test this hypothesis, we synthesized (*rac*)-**8** and (*rac*)-**9**, which respectively feature a *p*-nitro or *p*-amino moiety at this position. Indeed, both show improved affinities over that of (*rac*)-**2**, suggesting that an amino group is better suited than a nitro group. The indicated trend is further confirmed by (*rac*)-**10** and (*rac*)-**11**. Compounds (*rac*)-**12** and (*rac*)-**13** were synthesized with a polarizable bromine substituent at this position. Molecule (*rac*)-**12** does not improve affinity to both Plms within the estimated error of the assay. Likewise, (*rac*)-**13** is not beneficial for binding to Plm IV, whereas, interestingly, better binding to Plm II is observed.

Overall, for Plm IV, similar trends are observed as those for Plm II, strongly supporting our initial hypothesis that Plm IV is also capable of adopting a conformation with an open binding pocket as observed for Plm II (1LF2). The affinities measured for cathepsin D are all in the high micromolar range, which indicates satisfactory selectivity toward Plm II and IV.

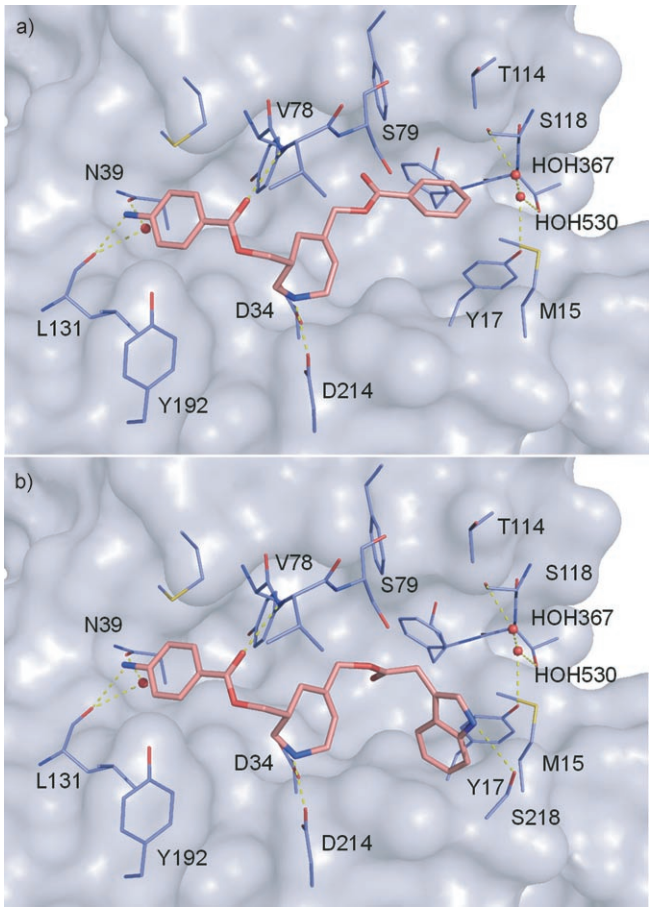

Figure 5. Minimized docking solutions of a) (*R*)-**1** and b) (*R*)-**5** in 1LF2. The protein is shown in blue, both ligands in salmon, color coded by atom type. Image created using PyMol 0.99.[59]

Chemical synthesis

N-Boc-2,3,4,7-tetrahydroazepine (*rac*)-**14**, bearing two anchoring groups, the unprotected hydroxymethyl function at position 3 as well as the TBDMS-protected group at position 5, is easily accessible by a straightforward convergent strategy in seven steps with 21% overall yield.[39] Condensation of the primary hydroxy group with either benzoyl chloride or *p*-nitrobenzoic acid applying standard procedures readily renders the ester derivatives (*rac*)-**15** and (*rac*)-**16**. Selective cleavage of the TBDMS group furnishes the respective hydroxymethyl derivatives (*rac*)-**17** and (*rac*)-**18**. These were subsequently condensed with a set of preliminarily chosen aromatic carboxylic acids to give the bis-ester derivatives (*rac*)-**19**–**23**. In the final synthetic step leading to the first series of inhibitors (*rac*)-**1**, (*rac*)-**4**, (*rac*)-**5**, (*rac*)-**9**, and (*rac*)-**13**, the nitro groups of the substituents in (*rac*)-**19**–**23** were reduced to the corresponding amino functionalities using tin(II) chloride in ethyl acetate at elevated temperature. Concomitantly with this reaction step, the *N*-Boc protecting groups were also removed, and after treatment with anhydrous HCl in Et_2O, the corresponding hydrochlorides (*rac*)-**1**, (*rac*)-**4**, (*rac*)-**5**, (*rac*)-**9**, and (*rac*)-**13** were obtained. For a second series of inhibitors, the Boc protecting group of the nitro compounds (*rac*)-**19**–**23** was directly cleaved under nonaqueous conditions to afford inhibitors (*rac*)-**3**, (*rac*)-**6**–**8**, and (*rac*)-**12** as their hydrochloride salts in good overall yield. Starting from the Boc-protected bis-diol (*rac*)-**24**, which can be obtained by deprotection of TBDMS-protected azepine (*rac*)-**14**, the bis-*p*-nitrophenylester (*rac*)-**25** is accessible in a one-step procedure. This precursor (*rac*)-**25** provides direct and easy access to further inhibitors either by simple cleavage of the Boc protecting group to give inhibitor (*rac*)-**10**, or by reduction of both nitro groups and subsequent Boc group deprotection to provide inhibitor (*rac*)-**11** as its trihydrochloride.

Conclusions

In summary, we have developed novel nonpeptidic Plm II and Plm IV inhibitors that feature a 2,3,4,7-tetrahydro-1*H*-azepine scaffold as core element. Equipped with suitable side chains to address two of the enzyme's specificity pockets, these inhibitors show activity in the nanomolar range. Derived from a combined subpocket search and a combinatorial docking approach, initial inhibitors with affinities in the low micromolar range were identified. These were subsequently synthesized by following our previously established synthetic route, which is mainly based on commercially available, inexpensive starting materials. Structural modifications of the initial lead structure in a consecutive design cycle indeed led to inhibitors that exhibit affinities in the sub-micromolar range. Overall, 13 inhibitors were synthesized, the experimentally determined K_i values of which are generally in good agreement with the design hypothesis. The determined structure–activity relationships, therefore, support our predicted binding mode for Plm II and Plm IV. Notably, as compound (*rac*)-**4** inhibits Plm II and Plm IV equally well and displays selectivity over human cathepsin D, this inhibitor represents our new lead structure. Future work will address an additional substrate recognition pocket to further increase affinity toward Plm II and Plm IV, and to retain or even increase the selectivity against cathepsin D.

Experimental Section

Assays and K_i determinations: Plm II activity assays were performed in 96-well microtiter plates with a Tecan Spectra Fluor spectrometer ($\lambda_{ex}=360$ nm, $\lambda_{em}=465$ nm). The fluorogenic substrate Arg-Gln-Phe*Nphe-Ile-Thr was purchased from Bachem (* denotes the cleavage site; Nphe = *p*-nitrophenylalanine). A 1 mM substrate stock solution in DMSO was prepared. The stock solution was diluted in a ratio of 1:50 with an acetic acid/acetate buffer (0.1 M, pH 4.5). This solution was distributed to the wells (180 μL each). The Plm II concentration, measured by UV/Vis, was 10 nM in an acetic acid/acetate buffer (0.1 M, pH 4.5). For the assay, protein (18 μL) was mixed with inhibitor (2 μL, dissolved in DMSO) and allowed to fully equilibrate with enzyme for 5 min. DMSO (2.3% final concentration) was used to guarantee complete dissolution of the inhibitors. For the reaction, the 20 μL enzyme inhibitor solution was added to the 180 μL substrate solution. The final enzyme concentration was 1 nM, and the final substrate concentration was 18 μM. Substrate conversion was recorded as an increase in fluorescence intensity over a period of 3 min, during which the intensity increased linearly with time. IC_{50} values were taken from plots of V_i/V_0 as a function of inhibitor concentration, for which V_i and V_0 are the initial rates of reaction in presence and absence of the inhibitor, respectively. To convert IC_{50} values to K_i values, the following equation was applied:

$$K_i = [IC_{50} - (E_t/2)][1 + (S/K_M)]^{-1}$$

for which E_t is the total enzyme concentration (1 nM), K_M is the Michaelis–Menten constant (63 μM), and S is the substrate concentration (18 μM).

Plm IV activity assays were essentially performed as described for Plm II. The enzyme concentration was 10 nM, $K_M=28$ μM, and S = 18 μM. Cathepsin D activity assays were essentially performed as described for Plm II. The enzyme concentration was 1 nM, $K_M=16$ μM, and S = 9 μM. The estimated error range for the assays is ±40%.

Homology model of Plm IV: As template for homology modeling, the complex structure of Plm II (1LF2) was used, assuming that Plm IV can also adopt a more open binding pocket. The sequence of Plm IV was initially mapped onto that of Plm II using the align option in MOE.[50] The sequences aligned with 69.3% identity (using the BLOSUM 62 substitution matrix[51]). The homology modeling of Plm IV was carried out in MOE version 2006.08.[50] Ten models were generated, and each was slightly minimized. The protein report of MOE was checked for outliers in the final model.

Molecular dynamics simulation: The MD simulation and all setup steps were performed with the Amber 8.0 suite of programs[52] using the Amber 1999 force field. The Plm structure with PDB code 1LEE was used as starting point. The ligand and all crystallographic water molecules were removed, and hydrogen atoms were added with PROTONATE. After estimating protonation states of all histidine residues and of the two catalytic aspartates (D34 and D214) at pH 5 with Poisson–Boltzmann pK_a calculations, histidines were set to the protonated form, and the two catalytic aspartates to the deprotonated form. The protein was initially subjected to 200 steps of minimization using a generalized Born solvation model. Subsequently, the system was solvated in a box of ~10300

TIP3P water molecules,[53] and sodium ions were added to ensure neutrality. After 200 steps of minimization of the solvated system, the MD simulation was started by heating the solvent to 300 K over a period of 20 ps and cooling to 100 K over 5 ps, keeping the protein fixed. Then the entire system was brought to 300 K over a period of 25 ps, and the simulation was continued for 10 ns under NPT conditions, using a time step of 2 fs and PME[54] for evaluating the electrostatic interactions. Energy data were saved every 20 fs, and protein coordinates every 0.5 ps. CARNAL was used for further analysis of the trajectory, and VMD 1.8.2[55] for visualization.

Computational docking: Docking studies were performed with the docking program FlexX (version 2.0.3).[56] The crystal structures of Plm II with PDB codes 1LF2, 1SME, and 2BJU were used as starting geometries. The ligand and all crystallographic water molecules were removed. For the active site determination, a radius of 13 Å was selected, always using complete amino acids. A fragment dataset with 2083 carboxylic acids was compiled from the Sigma–Aldrich catalogue, all with $M_r < 250$ Da. The core and the R group instances were preprocessed with Sybyl[57] as follows: correct atom and bond types as well as formal charges were assigned, hydrogen atoms were added, 3D structures were generated and energy minimized. All fragments were marked with an attachment point X. The core structure was marked with an attachment point R1. Then the core and the fragments were linked, and the connecting X and R atoms were removed from the atom list; a library of 2083 esters was generated.[40] The compounds were subsequently docked by using the *placeseq* option. During placement, the FlexX scoring function was applied for the final selection of the best-scored docking solutions.

Comparison of protein subpockets: The crystal structure of Plm II with PDB code 1LEE was used as starting geometry. All amino acids within 6 Å of the ligand were used for the determination of the binding pocket. The complete pocket was then further divided into subpockets. The S1 pocket (residues I14, M15, Y17, L32, D34, Y77, S79, F111, T114, S118, F120, I123, D214, S215, G216, and S218) and the S2′ pocket (residues S37, A38, N39, M75, N76, Y77, V78, L131, S132, and I133) were further analyzed. Cavbase,[47] a database developed from the database Relibase,[58] was used to compare the protein subpockets of Plm II with the subpockets of all stored binding pockets. All fragments which bind to similar subpockets were extracted.

General synthetic procedures: Reported yields refer to the analytically pure product obtained by column chromatography. All ^{1}H and ^{13}C NMR spectra were recorded on a Jeol Eclipse+ 500 MHz spectrometer (^{1}H NMR: 500 MHz, ^{13}C NMR: 125 MHz). Chemical shifts are reported in parts per million (ppm) and were referenced to TMS at 0.00 ppm (^{1}H) except for spectra of compounds containing a silyl protecting group, which were referenced to the residual $CHCl_3$ in $CDCl_3$ at 7.24 ppm. ^{13}C NMR spectra were referenced to $CDCl_3$ at 77.0 ppm or [D_6]DMSO at 39.5 ppm. NMR spectra were recorded in $CDCl_3$ unless otherwise indicated. Abbreviations: bdd = broad doublet of doublets, bm = broad multiplet, bs = broad singlet, d = doublet, m = multiplet, sm = symmetric multiplet, quint = quintet, q = quartet, s = singlet, t = triplet, ps = pseudo. MS data were obtained from a double-focusing sector field spectrometer type 7070 H (Vacuum Generators) or by a double-focusing sector field spectrometer type VG-AutoSpec (Micromass). Combustion analyses were determined on a Vario Micro Cube (Elementar Analysen, GmbH). Melting points were determined on a Mettler Toledo FP62 instrument and are uncorrected. Flash column chromatography was performed using silica gel 60 (0.05–0.1 mm) or silica gel 60 (0.04–0.063 mm) purchased from Macherey–Nagel. TLC was carried out using aluminum plates (0.2 mm) coated with silica gel 60 F_{254} (Merck), and the products were visualized by UV detection, iodine, or by phosphormolybdic acid ("blue stain"). Solvents and reagents that are commercially available were used without further purification unless otherwise noted. THF was dried by distillation from sodium/benzophenone. All moisture-sensitive reactions were carried out using oven-dried glassware under a positive stream of argon. Compounds **2**, **14**, and **24** were prepared according to published methods.[39]

(*R*,*S*)-5-(*tert*-Butyldimethylsilanyloxymethyl)-3-(4-nitrobenzoyloxymethyl)-2,3,4,7-tetrahydroazepine-1-carboxylic acid *tert*-butyl ester [(*rac*)-15]: *p*-Nitrobenzoic acid (0.281 g, 1.68 mmol, 1.2 equiv) and DMAP (0.009 g, 0.07 mmol, 5 mol%) were added to a stirred solution of (*rac*)-**14** (0.520 g, 1.40 mmol, 1.0 equiv) in a 1:1 mixture of THF and CH_2Cl_2 (20 mL) followed by the addition of a solution of DIC (0.229 g, 1.82 mmol, 1.3 equiv) in the above solvent mixture (5 mL) at room temperature. The reaction mixture was stirred for 12 h and then carefully quenched by the addition of a saturated $NaHCO_3$ solution (30 mL). After addition of Et_2O (50 mL), the layers were separated. The organic layer was filtered, and the residue was washed three times with Et_2O. The combined filtrates were washed twice with brine, dried over $MgSO_4$, filtered, and concentrated under reduced pressure. Column chromatography (hexanes/*t*BuOMe: 1:1) afforded 0.519 g (71%) of (*rac*)-**15** as a yellow oil: ^{1}H NMR: $\delta = 8.27$ (d, ^3J(H,H) = 8.3 Hz, 2H), 8.20 (d, ^3J(H,H) = 8.5 Hz, 2H), 5.73 (bs, 1H), 4.26 (d, ^3J(H,H) = 6.6 Hz, 2H), 3.97 (s, 2H), 4.08–3.89 (m, 2H), 3.70–3.59 (m, 1H), 3.48 (sm, 1H), 2.46–2.34 (bm, 1H), 2.31–2.20 (bt, 1H), 2.13 (dd, ^2J(H,H) = 14.8, ^3J(H,H) = 8.6 Hz, 1H), 1.42 (s, 9H), 0.86 (s, 9H), 0.02 ppm (s, 6H); ^{13}C NMR (rotamers): $\delta =$ 164.4, 155.4, 155.1, 150.5, 139.9, 138.9, 135.5, 135.4, 130.7, 130.6, 123.5, 122.2, 122.1, 79.7, 79.5, 67.8, 67.7, 67.4, 49.2, 49.1, 46.3, 36.9, 36.5, 29.3, 28.8, 28.4, 28.3, 25.8, 18.3, −5.37, −5.43 ppm; MS (ES+) *m/z* (%): 543 (46) $[M+Na]^+$, 1063 (100) $[2M+Na]^+$; HRMS (ES+): *m/z* calcd for $C_{26}H_{41}N_2O_7Si$: 521.268306, found: 521.270468.

(*R*,*S*)-3-Benzoyloxymethyl-5-(*tert*-butyldimethylsilanyloxymethyl)-2,3,4,7-tetrahydroazepine-1-carboxylic acid *tert*-butyl ester [(*rac*)-16]: TEA (0.40 mL, 2.60 mmol, 1.3 equiv) and a catalytic amount of DMAP were added to a stirred solution of (*rac*)-**14** (0.743 g, 2.0 mmol, 1.0 equiv) in CH_2Cl_2 (20 mL), followed by the dropwise addition of a solution of benzoyl chloride (0.3 mL, 2.20 mmol, 1.1 equiv in CH_2Cl_2 [2 mL]) at 0 °C. The reaction mixture was allowed to reach room temperature and was stirred for 18 h at ambient temperature. After addition of *t*BuOMe (50 mL), the solution was quenched with a saturated NH_4Cl solution, and the aqueous layer was extracted twice with *t*BuOMe (50 mL). The combined organic layers were washed with brine, dried over $MgSO_4$, filtered, and concentrated under reduced pressure. Column chromatography (hexanes/*t*BuOMe: 9:1) of the remaining oily residue afforded 0.688 g (72%) of (*rac*)-**16** as a colorless oil: ^{1}H NMR: $\delta = 8.02$ (dd, ^3J(H,H) = 8.3, ^4J(H,H) = 1.2 Hz, 2H), 7.54 (sm, 1H), 7.42 (pst, 2H), 5.73 (s, 1H), 4.20 (d, ^3J(H,H) = 6.9 Hz, 2H), 4.05–3.86 (m, 2H), 3.97 (s, 2H), 3.76–3.61 (m, 1H), 3.44 (dd, ^2J(H,H) = 14.2, ^3J(H,H) = 7.8 Hz, 1H), 2.45–2.30 (bd, 1H), 2.25 (pst, 1H), 2.17–2.08 (m, 1H), 1.42 (s, 9H), 0.87 (s, 9H), 0.02 ppm (s, 6H); ^{13}C NMR (rotamers): $\delta = 166.3$, 155.4, 155.2, 140.1, 139.2, 132.95, 132.86, 130.1, 129.6, 128.3, 122.0, 121.9, 79.7, 79.4, 67.7, 67.3, 66.91, 66.85, 49.5, 49.4, 46.2, 37.0, 36.6, 29.4, 29.0, 28.4, 25.9, 18.3, −5.46, −5.43 ppm; MS (ES+) *m/z* (%): 498 (77) $[M+Na]^+$, 973 (100) $[2M+Na]^+$; HRMS (ES+): *m/z* calcd for $C_{26}H_{42}NO_5Si$: 476.283227, found: 476.284998; Anal. calcd for $C_{26}H_{41}NO_5Si$: C 65.65, H 8.69, N 2.94, found: C 65.64, H 8.75, N 2.87.

(*R*,*S*)-5-Hydroxymethyl-3-(4-nitrobenzoyloxymethyl)-2,3,4,7-tetrahydroazepine-1-carboxylic acid *tert*-butyl ester [(*rac*)-17]: Com-

pound (*rac*)-**15** (0.437 g, 0.84 mmol, 1.0 equiv) was dissolved in 15 mL of a 30:1 mixture of THF and aqueous HCl 32% and stirred at room temperature for 30 min. After addition of a saturated $NaHCO_3$ solution (15 mL), the reaction mixture was extracted three times with Et_2O. The combined organic layers were washed with brine, dried over $MgSO_4$, filtered, and concentrated under reduced pressure. Column chromatography (hexanes/*t*BuOMe: 1:1) afforded 0.263 g (77%) of (*rac*)-**17** as a colorless oil: ^{1}H NMR: $\delta = 8.30$ (d, $^3J(H,H) = 8.7$ Hz, 2H), 8.22 (d, $^3J(H,H) = 8.9$ Hz, 2H), 5.80 (s, 1H), 4.30 (d, $^3J(H,H) = 6.6$ Hz, 2H), 4.09–3.95 (m, 2H), 4.02 (s, 2H), 3.72–3.63 (m, 1H), 3.60–3.50 (m, 1H), 2.51–2.41 (m, 1H), 2.38 (d, $^2J(H,H) = 15.0$ Hz, 1H), 2.26 (dd, $^2J(H,H) = 15.2$, $^3J(H,H) = 8.6$ Hz, 1H), 1.45 ppm (s, 9H); ^{13}C NMR (rotamers): $\delta = 164.4$, 155.3, 155.2, 150.5, 140.2, 139.7, 135.4, 135.3, 130.6, 130.5, 123.4, 123.2, 123.1, 79.9, 79.7, 67.7, 67.5, 49.3, 49.1, 46.3, 46.0, 36.9, 36.5, 29.4, 29.2, 28.3 ppm; MS (ES+) *m/z* (%) 429 (100) $[M+Na]^+$, 835 (80) $[2M+Na]^+$; HRMS (ES+): *m/z* calcd for $C_{20}H_{26}N_2O_7Na$: 429.163771, found: 429.161823; Anal. calcd for $C_{20}H_{26}N_2O_7$: C 59.10, H 6.45, N 6.89, found: C 59.04, H 6.56, N 6.82.

(*R*,*S*)-3-Benzoyloxymethyl-5-hydroxymethyl-2,3,4,7-tetrahydroazepine-1-carboxylic acid *tert*-butyl ester [(*rac*)-18]: Compound (*rac*)-**16** (0.618 g, 1.30 mmol, 1.0 equiv) was dissolved in 20 mL of a 30:1 mixture of THF and aqueous HCl 32% and stirred at room temperature for 30 min. After addition of a saturated $NaHCO_3$ solution (20 mL), the reaction mixture was extracted three times with Et_2O. The combined organic layers were washed with brine, dried over $MgSO_4$, filtered, and concentrated under reduced pressure. Column chromatography (hexanes/*t*BuOMe: 1:1) afforded 0.423 g (90%) of (*rac*)-**18** as a colorless oil: ^{1}H NMR: $\delta = 8.04$ (dd, $^3J(H,H) = 8.3$, $^4J(H,H) = 1.0$ Hz, 2H), 7.57 (t, $^3J(H,H) = 7.1$ Hz, 1H), 7.44 (t, $^3J(H,H) = 7.6$ Hz, 2H), 5.78 (bs, 1H), 4.24 (d, $^3J(H,H) = 6.2$ Hz, 2H), 4.08–3.94 (m, 2H), 4.01 (s, 2H), 3.77–3.63 (m, 1H), 3.49 (sm, 1H), 2.51–2.39 (m, 1H), 2.36 (d, $^2J(H,H) = 15.3$ Hz, 1H), 2.26 (sm, 1H), 1.45 ppm (s, 9H); ^{13}C NMR (rotamers): $\delta = 166.4$, 155.3, 140.4, 140.0, 133.0, 132.9, 129.9, 129.4, 128.3, 123.0, 122.8, 79.9, 79.8, 67.7, 67.5, 66.8, 66.6, 49.5, 49.3, 46.2, 46.1, 37.0, 36.5, 29.4, 28.3 ppm; MS (ES+) *m/z* (%): 384 (25) $[M+Na]^+$, 745 (100) $[2M+Na]^+$; HRMS (ES+) *m/z* calcd for $C_{20}H_{27}NO_5Na$: 384.178693, found: 384.176482; Anal. calcd for $C_{20}H_{27}NO_5$: C 66.46, H 7.53, N 3.88, found: C 66.69, H 7.56, N 4.06.

(*R*,*S*)-5-Benzoyloxymethyl-3-(4-nitrobenzoyloxymethyl)-2,3,4,7-tetrahydroazepine-1-carboxylic acid *tert*-butyl ester [(*rac*)-19]: TEA (0.06 mL, 0.42 mmol, 1.3 equiv) and a catalytic amount of DMAP were added to a stirred solution of (*rac*)-**17** (0.130 g, 0.32 mmol, 1.0 equiv) in CH_2Cl_2 (5 mL) at 0 °C. The reaction mixture was allowed to reach room temperature followed by the dropwise addition of a solution of benzoyl chloride (0.04 mL, 0.35 mmol, 1.1 equiv) in CH_2Cl_2 (0.5 mL). The mixture was stirred for 14 h at ambient temperature. After addition of *t*BuOMe (10 mL), the reaction mixture was quenched with a saturated NH_4Cl solution (10 mL), and the aqueous layer was extracted twice with *t*BuOMe. The combined organic layers were washed with brine, dried over $MgSO_4$, filtered, and concentrated under reduced pressure. Column chromatography (hexanes/*t*BuOMe: 4:1) afforded 0.142 g (87%) of (*rac*)-**19** as colorless oil: ^{1}H NMR: $\delta = 8.20$ (sm, 2H), 8.13 (sm, 2H), 8.01 (d, $^3J(H,H) = 7.6$ Hz, 2H), 7.58–7.52 (m, 1H), 7.45–7.38 (m, 2H), 5.96–5.89 (m, 1H), 4.74 (s, 2H), 4.40–4.34 (m, 1H), 4.26 (dd, $^2J(H,H) = 11.0$, $^3J(H,H) = 7.3$ Hz, 1H), 4.17–3.95 (m, 2H), 3.75–3.65 (m, 1H), 3.60–3.49 (m, 1H), 2.60–2.43 (m, 2H), 2.34 (dd, $^2J(H,H) = 15.4$, $^3J(H,H) = 8.7$ Hz, 1H), 1.45 ppm (s, 9H); ^{13}C NMR (rotamers): $\delta =$ 166.1, 164.3, 155.3, 155.0, 150.4, 135.5, 135.2, 135.1, 134.5, 133.0, 130.5, 129.8, 129.4, 128.3, 127.5, 127.3, 123.3, 80.0, 79.8, 69.4, 67.3, 48.9, 46.3, 37.0, 36.6, 29.7, 29.2, 28.3 ppm; MS (ES+) *m/z* (%): 533 (100) $[M+Na]^+$, 1043 (21) $[2M+Na]^+$; HRMS (ES+) *m/z* calcd for $C_{27}H_{31}N_2O_8$: 511.208041, found: 511.209535; Anal. calcd for $C_{27}H_{30}N_2O_8$: C 63.52, H 5.92, N 5.49, found: C 63.50, H 6.08, N 5.31.

General procedure for the synthesis of compounds (*rac*)-**20**–**22:** The appropriate carboxylic acid (1.2 equiv) and DMAP (5 mol%) were added to a stirred solution of alcohol (*rac*)-**17** (1.0 equiv) in a 1:1 mixture of THF and CH_2Cl_2, followed by the addition of a solution of DIC (1.3 equiv) in the above solvent mixture. The reaction mixture was stirred at room temperature until TLC indicated the completion of the reaction and was then carefully quenched by addition of a saturated $NaHCO_3$ solution. After addition of Et_2O, the layers were separated. The organic layer was filtered, and the residue was washed three times with Et_2O. The combined filtrates were washed twice with brine, dried over $MgSO_4$, filtered, and concentrated under reduced pressure.

(*R*,*S*)-5-(2-1*H*-Indol-3-ylacetoxymethyl)-3-(4-nitrobenzoyloxymethyl)-2,3,4,7-tetrahydroazepine-1-carboxylic acid *tert*-butyl ester [(*rac*)-20]: Reaction of (*rac*)-**17** (0.691 g, 1.70 mmol, 1.0 equiv) with 3-indole acetic acid (0.357 g, 2.04 mmol, 1.2 equiv) and subsequent column chromatography (hexanes/*t*BuOMe: 3:2) yielded 0.805 g (84%) of (*rac*)-**20** as a yellow, hygroscopic solid: ^{1}H NMR: $\delta = 8.22$ (d, $^3J(H,H) = 8.3$ Hz, 2H), 8.20 (bs, 1H), 8.15 (d, $^3J(H,H) = 7.3$ Hz, 2H), 7.57 (d, $^3J(H,H) = 8.0$ Hz, 1H), 7.34–7.29 (m, 1H), 7.18–7.13 (m, 2H), 7.09 (dt, $^3J(H,H) = 7.3$, $^4J(H,H) = 0.9$ Hz, 1H), 5.80–5.75 (m, 1H), 4.51 (s, 2H), 4.20–4.04 (m, 2H), 4.04–3.85 (m, 2H), 3.78 (s, 2H), 3.66–3.53 (m, 1H), 3.49–3.38 (m, 1H), 2.32–2.19 (m, 2H), 2.19–2.10 (m, 1H), 1.44 ppm (s, 9H); ^{13}C NMR (rotamers): $\delta = 171.7$, 164.5, 155.4, 155.1, 150.5, 150.4, 136.0, 135.5, 135.2, 134.5, 130.6, 127.5, 127.2, 127.0, 123.5, 123.1, 122.1, 119.5, 118.6, 111.2, 108.1, 80.1, 79.9, 69.3, 67.4, 49.0, 46.2, 36.7, 36.3, 31.3, 29.7, 29.1, 28.4 ppm; MS (ES+) *m/z* (%): 586 (100) $[M+Na]^+$, 1149 (35) $[2M+Na]^+$; HRMS (ES+) *m/z* calcd for $C_{30}H_{33}N_3O_8Na$: 586.216535, found: 586.213797.

(*R*,*S*)-5-(Naphthalene-1-carbonyloxymethyl)-3-(4-nitrobenzoyloxymethyl)-2,3,4,7-tetrahydroazepine-1-carboxylic acid *tert*-butyl ester [(*rac*)-21]: (*rac*)-**21** was obtained from (*rac*)-**17** (1.016 g, 2.50 mmol, 1.0 equiv) and 1-naphthoic acid (0.517 g, 3.00 mmol, 1.2 equiv). Column chromatography (hexanes/*t*BuOMe: 3:1) gave 0.620 g (44%) of (*rac*)-**21** as a yellow solid: mp: 117 °C; ^{1}H NMR: $\delta = 8.84$ (t, $^3J(H,H) = 7.5$ Hz, 1H), 8.17–8.12 (m, 1H), 8.03–7.92 (m, 5H), 7.83 (dd, $^3J(H,H) = 8.2$, $^3J(H,H) = 7.8$ Hz, 1H), 7.57 (sm, 1H), 7.51 (sm, 1H), 7.44 (sm, 1H), 6.02–5.96 (bd, 1H), 4.83 (sm, 2H), 4.37 (sm, 1H), 4.27–4.19 (m, 1H), 4.18–4.05 (m, 1H), 4.03 (sm, 1H), 3.70 (sm, 1H), 3.50 (sm, 1H), 2.60–2.50 (m, 2H), 2.45–2.36 (m, 1H), 1.48 ppm (s, 9H); ^{13}C NMR (rotamers): $\delta = 166.9$, 164.2, 155.4, 155.1, 150.1, 135.7, 135.0, 134.8, 134.7, 133.7, 133.5, 131.2, 130.3, 130.2, 130.1, 128.4, 127.9, 127.8, 126.5, 126.2, 125.5, 124.4, 123.2, 80.1, 79.9, 69.7, 67.2, 67.1, 49.0, 46.5, 37.0, 36.7, 29.7, 29.2, 28.4 ppm; MS (ES+) *m/z* (%): 583 (100) $[M+Na]^+$, 1143 (40) $[2M+Na]^+$; HRMS (ES+) *m/z* calcd for $C_{31}H_{32}N_2O_8Na$: 583.205636, found: 583.208517; Anal. calcd for $C_{31}H_{32}N_2O_8$: C 66.42, H 5.75, N 5.00, found: C 66.13, H 5.89, N 4.83.

(*R*,*S*)-5-(4-Bromobenzoyloxymethyl)-3-(4-nitrobenzoyloxymethyl)-2,3,4,7-tetrahydroazepine-1-carboxylic acid *tert*-butyl ester [(*rac*)-22]: Reaction of (*rac*)-**17** (1.016 g, 2.5 mmol, 1.0 equiv) with 4-bromobenzoic acid (0.603 g, 3.0 mmol, 1.2 equiv) gave 0.860 g (58%) of (*rac*)-**22** as a yellow oil after column chromatography (hexanes/*t*BuOMe: 2:1): ^{1}H NMR (rotamers): $\delta = 8.24$ (d, $^3J(H,H) = 8.0$ Hz, 2H), 8.14 (dd, $^3J(H,H) = 9.6$, $^3J(H,H) = 8.7$ Hz, 2H), 7.85 (d, $^3J(H,H) = 7.8$ Hz, 2H), 7.56–7.50 (m, 2H), 5.93–5.90 (m, 1H), 4.77–

4.66 (m, 2H), 4.39–4.32 (m, 1H), 4.29–4.21 (m, 1H), 4.15–3.95 (m, 2H), 3.74–3.64 (m, 1H), 3.59–3.46 (m, 1H), 2.57–2.41 (m, 2H), 2.33 (dd, ^2J(H,H) = 15.4, ^3J(H,H) = 8.5 Hz, 1H), 1.46 ppm (s, 9H); ^{13}C NMR (rotamers): δ = 165.5, 164.4, 155.4, 155.1, 150.5, 135.3, 135.2, 134.3, 131.7, 131.0, 130.6, 130.5, 128.7, 128.2, 127.8, 127.7, 123.4, 80.1, 79.9, 69.8, 67.4, 49.1, 49.0, 46.4, 37.0, 36.7, 29.8, 29.3, 28.4 ppm; MS (ES+) *m/z* (%): 613 (100) $[M+Na]^+$; HRMS (ES+) *m/z* calcd for $C_{27}H_{29}BrN_2O_8Na$: 611.100497, found: 611.103088; Anal. calcd for $C_{27}H_{29}BrN_2O_8$: C 55.02, H 4.96, N 4.75, found: C 54.69, H 5.01, N 4.78.

(*R*,*S*)-3-Benzoyloxymethyl-5-(4-nitrobenzoyloxymethyl)-2,3,4,7-tetrahydroazepine-1-carboxylic acid *tert*-butyl ester [(*rac*)-**23**]: *p*-Nitrobenzoic acid (0.224 g, 1.34 mmol, 1.2 equiv) and DMAP (0.007 g, 0.06 mmol, 5 mol%) were added to a stirred solution of (*rac*)-**18** (0.405 g, 1.12 mmol, 1.0 equiv) in a 1:1 mixture of THF and CH_2Cl_2 (20 mL), followed by the addition of a solution of DIC (0.23 mL, 1.50 mmol, 1.3 equiv) in the above solvent mixture (5 mL). The solution was stirred at room temperature for 18 h and then carefully quenched by addition of saturated $NaHCO_3$ solution (30 mL). After addition of Et_2O (50 mL), the layers were separated. The organic layer was filtered, and the residue was washed three times with Et_2O (50 mL). The combined filtrates were washed twice with brine, dried over $MgSO_4$, filtered, and concentrated under reduced pressure. Column chromatography (hexanes/*t*BuOMe: 1:1) afforded 0.371 g (65%) of (*rac*)-**23** as a yellow oil: ^{1}H NMR: δ = 8.20 (d, ^3J(H,H) = 8.7 Hz, 2H), 8.15 (d, ^3J(H,H) = 8.9 Hz, 2H), 7.98 (d, ^3J(H,H) = 7.6 Hz, 2H), 7.54 (dd, ^3J(H,H) = 7.3, ^3J(H,H) = 6.9 Hz, 1H), 7.40 (t, ^3J(H,H) = 7.6 Hz, 2H), 5.97–5.87 (m, 1H), 4.80 (d, ^2J(H,H) = 12.6 Hz, 1H), 4.74 (d, ^2J(H,H) = 12.4 Hz, 1H), 4.35–4.27 (m, 1H), 4.21 (dd, ^2J(H,H) = 11.0, ^3J(H,H) = 7.1 Hz, 1H), 4.14–3.97 (m, 2H), 3.78–3.66 (m, 1H), 3.50 (dd, ^2J(H,H) = 14.2, ^3J(H,H) = 8.0 Hz, 1H), 2.52–2.44 (m, 2H), 2.39–2.30 (m, 1H), 1.43 ppm (s, 9H); ^{13}C NMR (rotamers): δ = 166.1, 164.2, 155.2, 155.1, 150.4, 135.1, 135.0, 134.2, 133.0, 130.5, 129.7, 129.3, 128.2, 128.1, 123.4, 80.0, 79.7, 70.4, 66.5, 66.3, 49.2, 49.0, 46.2, 37.1, 36.7, 29.7, 29.5, 28.3 ppm; MS (ES+) *m/z* (%): 533 (78) $[M+Na]^+$, 1043 (100) $[2M+Na]^+$; HRMS (ES+) *m/z* calcd for $C_{27}H_{30}N_2O_8Na$: 533.189986, found: 533.191940; Anal. calcd for $C_{27}H_{30}N_2O_8$: C 63.52, H 5.92, N 5.49, found: C 63.34, H 5.99, N 5.50.

General procedure for the preparation of compounds (*rac*)-**1**, (*rac*)-**4**, (*rac*)-**5**, (*rac*)-**9**, (*rac*)-**11**, and (*rac*)-**13**: $SnCl_2{\cdot}2H_2O$ (5.0 equiv) was added to a solution of the appropriate *p*-nitrobenzoyloxymethyl derivative ((*rac*)-**19**–**23**, (*rac*)-**25**, 1.0 equiv) in EtOAc. The reaction mixture was stirred for 3 h at 80 °C and then allowed to reach room temperature. The reaction was quenched through careful addition of a saturated $NaHCO_3$ solution, until pH 7–8 was reached. The layers were separated, and the aqueous layer was extracted twice with EtOAc. The combined organic layers were washed twice with brine, dried over $MgSO_4$, filtered, and concentrated under reduced pressure. After column chromatography, the oily residue was treated with HCl (20.0 equiv of a 2.0 M solution in Et_2O) and stirred for 24 h at room temperature. The resulting precipitate was separated by filtration under a positive pressure of argon, thoroughly washed with dry Et_2O, and dried.

(*R*,*S*)-3-(4-Aminobenzoyloxymethyl)-5-benzoyloxymethyl-2,3,4,7-tetrahydro-1*H*-azepine hydrochloride [(*rac*)-**1**]: Following the general procedure, use of (*rac*)-**19** (0.150 g, 0.294 mmol, 1.0 equiv) afforded 0.059 g (48%) of (*rac*)-**1** as a brownish solid after column chromatography (CH_2Cl_2/MeOH: 93:7): mp: 124 °C; ^{1}H NMR ([D$_6$]DMSO): δ = 7.98 (dd, ^3J(H,H) = 8.3, ^4J(H,H) = 1.0 Hz, 2H), 7.68–7.63 (m, 3H), 7.52 (t, ^3J(H,H) = 7.6 Hz, 2H), 6.53 (d, ^3J(H,H) = 8.7 Hz, 2H), 5.98 (s, 2H), 5.91 (dd, ^3J(H,H) = 5.5, ^3J(H,H) = 4.6 Hz, 1H), 4.76 (s, 2H), 4.12 (d, ^3J(H,H) = 6.2 Hz, 2H), 3.71–3.60 (m, 2H), 3.41–3.35 (m, 2H), 3.08 (dd, ^2J(H,H) = 13.0, ^3J(H,H) = 10.0 Hz, 1H), 2.41 (d, ^2J(H,H) = 15.6 Hz, 1H), 2.38–2.29 ppm (m, 1H); ^{13}C NMR ([D$_6$]DMSO): δ = 165.6, 165.3, 153.6, 140.4, 133.4, 131.1, 129.4, 129.1, 128.7, 122.3, 115.4, 112.6, 68.2, 65.2, 50.2, 43.4, 34.2, 30.6 ppm; MS (ES+) *m/z* (%): 381 (100) $[M+H]^+$, 761 (9) $[2M+H]^+$; HRMS (ES+) *m/z* calcd for $C_{22}H_{25}N_2O_4$: 381.181433, found: 381.184246.

(*R*,*S*)-3-(4-Aminobenzoyloxymethyl)-5-(2-1*H*-indol-3-ylacetoxymethyl)-2,3,4,7-tetrahydro-1*H*-azepine hydrochloride [(*rac*)-**4**]: Following the general procedure, use of (*rac*)-**20** (0.099 g, 0.176 mmol, 1.0 equiv) afforded 0.043 g (52%) of (*rac*)-**4** as a brownish, hygroscopic solid after column chromatography (CH_2Cl_2/MeOH: 7:3): ^{1}H NMR ([D$_6$]DMSO): δ = 10.95 (bs, 1H), 8.48–8.15 (bs, 2H), 7.67 (d, ^3J(H,H) = 8.7 Hz, 2H), 7.48 (d, ^3J(H,H) = 7.8 Hz, 1H), 7.35 (d, ^3J(H,H) = 8.3 Hz, 1H), 7.24 (d, ^4J(H,H) = 2.3 Hz, 1H), 7.06 (t, ^3J(H,H) = 6.9 Hz, 1H), 6.97 (dd, ^3J(H,H) = 6.9, ^4J(H,H) = 0.9 Hz, 1H), 6.57 (d, ^3J(H,H) = 8.7 Hz, 2H), 5.99 (s, 2H), 5.76–5.71 (m, 1H), 4.51 (s, 2H), 4.04 (sm, 2H), 3.76 (s, 2H), 3.58 (t, ^3J(H,H) = 6.4 Hz, 2H), 3.36–3.32 (m, 1H), 3.05 (dd, ^2J(H,H) = 13.0, ^3J(H,H) = 10.2 Hz, 1H), 2.39 (dd, ^2J(H,H) = 15.9, ^3J(H,H) = 10.4 Hz, 1H), 2.24 (d, ^2J(H,H) = 15.6 Hz, 1H), 2.27–2.19 ppm (m, 1H); ^{13}C NMR ([D$_6$]DMSO): δ = 171.0, 165.6, 153.6, 140.6, 136.0, 131.1, 126.9, 124.0, 121.5, 121.0, 118.4, 118.3, 115.4, 112.6, 111.3, 106.7, 67.4, 65.1, 50.2, 43.3, 34.1, 30.6, 30.4 ppm; MS (ES+) *m/z* (%): 434 (100) $[M+H]^+$, 867 (7) $[2M+H]^+$; HRMS (ES+) *m/z* calcd for $C_{25}H_{28}N_3O_4$: 434.207982, found: 434.210643.

(*R*,*S*)-3-(4-Aminobenzoyloxymethyl)-5-(naphthalene-1-carbonyloxymethyl)-2,3,4,7-tetrahydro-1*H*-azepine hydrochloride [(*rac*)-**5**]: Following the general procedure, employment of (*rac*)-**21** (0.398 g, 0.71 mmol, 1.0 equiv) rendered 0.242 g (73%) of (*rac*)-**5** as a brownish solid after column chromatography (CH_2Cl_2/MeOH: 8:2): mp: 197 °C; ^{1}H NMR ([D$_4$]MeOH): δ = 8.84 (d, ^3J(H,H) = 8.7 Hz, 1H), 8.20 (dd, ^3J(H,H) = 7.2, ^4J(H,H) = 1.2 Hz, 1H), 8.10 (d, ^3J(H,H) = 8.3 Hz, 1H), 7.95 (d, ^3J(H,H) = 7.3 Hz, 1H), 7.69 (dt, ^3J(H,H) = 8.7, ^4J(H,H) = 2.3 Hz, 2H), 7.60 (ddd, ^3J(H,H) = 7.9, ^3J(H,H) = 7.6, ^4J(H,H) = 1.4 Hz, 1H), 7.55 (ddd, ^3J(H,H) = 7.5, ^3J(H,H) = 7.3, ^4J(H,H) = 1.2 Hz, 1H), 7.50 (dd, ^3J(H,H) = 7.7, ^4J(H,H) = 0.7 Hz, 1H), 6.53 (dt, ^3J(H,H) = 10.0, ^4J(H,H) = 1.8 Hz, 2H), 6.06 (t, ^3J(H,H) = 6.0 Hz, 1H), 4.91 (s, 2H), 4.24 (dd, ^2J(H,H) = 11.2, ^3J(H,H) = 6.4 Hz, 1H), 4.22 (dd, ^2J(H,H) = 11.2, ^3J(H,H) = 6.4 Hz, 1H), 3.84 (dd, ^2J(H,H) = 15.6, ^3J(H,H) = 6.2 Hz, 1H), 3.78 (dd, ^2J(H,H) = 15.6, ^3J(H,H) = 5.7 Hz, 1H), 3.58 (dd, ^2J(H,H) = 13.3, ^3J(H,H) = 9.6 Hz, 1H), 3.23 (dd, ^2J(H,H) = 13.3, ^3J(H,H) = 10.3 Hz, 1H), 2.64 (d, ^3J(H,H) = 6.0 Hz, 2H), 2.57–2.44 ppm (m, 1H); ^{13}C NMR ([D$_6$]DMSO): δ = 166.2, 165.6, 153.6, 140.7, 133.5, 133.4, 131.1, 130.4, 129.9, 128.7, 127.9, 126.34, 126.33, 125.0, 124.8, 122.3, 115.4, 112.6, 68.4, 65.2, 50.1, 43.2, 34.1, 30.7 ppm; MS (ES+) *m/z* (%): 431 (100) $[M+H]^+$, 861 (10) $[2M+H]^+$; HRMS (ES+) *m/z* calcd for $C_{26}H_{27}N_2O_4$: 431.197083, found: 431.194869; Anal. calcd for $C_{26}H_{27}N_2O_4Cl{\cdot}1/2H_2O$: C 65.61, H 5.93, N 5.89, found: C 65.82, H 5.93, N 5.76.

(*R*,*S*)-3-(4-Aminobenzoyloxymethyl)-5-(4-bromobenzoyloxymethyl)-2,3,4,7-tetrahydro-1*H*-azepine hydrochloride [(*rac*)-**13**]: Following the general procedure, employment of (*rac*)-**22** (0.212 g, 0.36 mmol, 1.0 equiv) provided 0.084 g (47%) of (*rac*)-**13** as a brownish solid after column chromatography (CH_2Cl_2/MeOH: 7:3): mp: 122 °C; ^{1}H NMR ([D$_6$]DMSO): δ = 9.61 (bs, 1H), 9.24 (bs, 1H), 7.90 (d, ^3J(H,H) = 8.0 Hz, 2H), 7.73 (d, ^3J(H,H) = 8.0 Hz, 2H), 7.68 (d, ^3J(H,H) = 8.3 Hz, 2H), 6.64 (d, ^3J(H,H) = 8.3 Hz, 2H), 5.91 (bs, 1H), 4.78 (s, 2H), 4.19–4.12 (sm, 2H), 3.82–3.66 (m, 2H), 3.44 (d, ^2J(H,H) = 12.0 Hz, 1H), 3.23–3.12 (m, 1H), 2.60–2.53 (m, 1H), 2.43 ppm (d, ^2J(H,H) = 14.9 Hz, 2H); ^{13}C NMR ([D$_6$]DMSO): δ = 165.4, 164.5, 151.4, 141.2, 131.8, 131.00, 130.97, 128.5, 127.4, 120.8, 116.9, 113.9, 68.1, 65.1, 49.5, 42.5, 33.4, 30.4 ppm; MS (ES+) *m/z* (%): 459 (100) $[M+H]^+$; HRMS (ES+) *m/z* calcd for $C_{22}H_{24}N_2O_4Br$:

459.091944, found: 459.091967; Anal. calcd for $C_{22}H_{24}N_2O_4BrCl\cdot4H_2O$: C 46.53, H 5.68, N 4.93, found: C 46.75, H 5.11, N 4.87.

(*R*,*S*)-5-(4-Aminobenzoyloxymethyl)-3-benzoyloxymethyl-2,3,4,7-tetrahydro-1*H*-azepine hydrochloride [(*rac*)-9]: Following the general procedure, use of (*rac*)-**23** (0.173 g, 0.339 mmol, 1.0 equiv) afforded 0.099 g (70%) of (*rac*)-**9** as a brownish solid after column chromatography (CH_2Cl_2/MeOH: 93:7): mp: 81 °C; ^{1}H NMR ([D$_6$]DMSO): δ = 7.97 (dd, ^3J(H,H) = 7.7, ^4J(H,H) = 1.2 Hz, 2H), 7.65 (m, 3H), 7.50 (t, ^3J(H,H) = 7.6 Hz, 2H), 6.56 (d, ^3J(H,H) = 8.7 Hz, 2H), 6.00 (s, 2H), 5.87 (t, ^3J(H,H) = 5.4 Hz, 1H), 4.64 (s, 2H), 4.24 (d, ^3J(H,H) = 6.2 Hz, 2H), 3.65 (dd, ^2J(H,H) = 16.0, ^3J(H,H) = 5.7 Hz, 1H), 3.59 (dd, ^2J(H,H) = 15.8, ^3J(H,H) = 5.5 Hz, 1H), 3.38 (dd, ^2J(H,H) = 13.1, ^3J(H,H) = 6.1 Hz, 1H), 3.11 (dd, ^2J(H,H) = 12.9, ^3J(H,H) = 9.8 Hz, 1H), 2.50–2.47 (m, 1H), 2.40 (d, ^2J(H,H) = 15.4 Hz, 1H), 2.41–2.33 ppm (m, 1H); ^{13}C NMR ([D$_6$]DMSO): δ = 165.5, 164.4, 153.6, 140.6, 133.3, 131.1, 129.5, 129.1, 128.7, 122.4, 115.4, 112.6, 67.1, 66.3, 50.5, 43.9, 34.4, 30.5 ppm; MS (ES+) *m/z* (%): 381 (100) $[M+H]^+$, 761 (10) $[2M+H]^+$; HRMS (ES+) *m/z* calcd for $C_{22}H_{25}N_2O_4$: 381.181433, found: 381.178897; Anal. calcd for $C_{22}H_{25}N_2O_4Cl\cdot1H_2O$: C 60.76, H 6.25, N 6.44, found: C 60.31, H 6.32, N 6.07.

General procedure for the preparation of compounds (*rac*)-**3**, (*rac*)-**6**, (*rac*)-**7**, (*rac*)-**8**, (*rac*)-**10**, and (*rac*)-**12:** A suspension of the appropriate Boc-protected derivative [(*rac*)-**19**–**23**, (*rac*)-**25**, 1.0 equiv] in a solution of HCl (20.0 equiv, 2.0 M in Et_2O) was stirred for 24 h at room temperature. The resulting precipitate was separated by filtration under a positive pressure of argon, thoroughly washed with dry Et_2O, and dried.

(*R*,*S*)-5-Benzoyloxymethyl-3-(4-nitrobenzoyloxymethyl)-2,3,4,7-tetrahydro-1*H*-azepine hydrochloride [(*rac*)-3]: According to the general procedure, employment of (*rac*)-**19** (0.100 g, 0.196 mmol) afforded 0.08 g (91%) of (*rac*)-**3** as a colorless solid: mp: 226 °C; ^{1}H NMR ([D$_6$]DMSO): δ = 9.47 (bs, 1H), 9.13 (bs, 1H), 8.29 (d, ^3J(H,H) = 8.7 Hz, 2H), 8.20 (d, ^3J(H,H) = 8.7 Hz, 2H), 7.98 (d, ^3J(H,H) = 7.3 Hz, 2H), 7.67 (t, ^3J(H,H) = 7.3 Hz, 1H), 7.51 (t, ^3J(H,H) = 7.6 Hz, 2H), 5.93 (t, ^3J(H,H) = 4.8 Hz, 1H), 4.82 (d, ^2J(H,H) = 13.5 Hz, 1H), 4.78 (d, ^2J(H,H) = 13.3 Hz, 1H), 4.33 (d, ^3J(H,H) = 5.7 Hz, 2H), 3.84–3.70 (m, 2H), 3.51 (bd, ^2J(H,H) = 13.5 Hz, 1H), 3.31–3.20 (m, 1H), 2.62 (dd, ^2J(H,H) = 15.6, ^3J(H,H) = 10.5 Hz, 1H), 2.50–2.40 ppm (m, 2H); ^{13}C NMR ([D$_6$]DMSO): δ = 165.4, 164.2, 150.4, 141.6, 134.9, 133.6, 130.8, 129.5, 129.3, 128.9, 123.9, 120.9, 68.0, 67.0, 49.6, 42.8, 33.4, 30.5 ppm; MS (ES+) *m/z* (%): 411 (100) $[M+H]^+$; HRMS (ES+) *m/z* calcd for $C_{22}H_{23}N_2O_6$: 411.155612, found: 411.156088; Anal. calcd for $C_{22}H_{23}N_2O_6Cl\cdot1H_2O$: C 56.84, H 5.42, N 6.03, found: C 57.00, H 5.12, N 5.88.

(*R*,*S*)-5-(2-1*H*-Indol-3-ylacetoxymethyl)-3-(4-nitrobenzoyloxymethyl)-2,3,4,7-tetrahydro-1*H*-azepine hydrochloride [(*rac*)-6]: Use of (*rac*)-**20** (0.105 g, 0.186 mmol) gave 0.079 g (85%) of (*rac*)-**6** as a yellow solid: mp: 165 °C; ^{1}H NMR ([D$_6$]DMSO): δ = 11.01 (s, 1H), 9.58 (bs, 1H), 9.23 (bs, 1H), 8.32 (d, ^3J(H,H) = 8.5 Hz, 2H), 8.22 (d, ^3J(H,H) = 8.5 Hz, 2H), 7.47 (d, ^3J(H,H) = 7.8 Hz, 1H), 7.33 (d, ^3J(H,H) = 8.0 Hz, 1H), 7.25 (s, 1H), 7.04 (t, ^3J(H,H) = 7.5 Hz, 1H), 6.96 (t, ^3J(H,H) = 7.3 Hz, 1H), 5.76 (s, 1H), 4.55 (s, 2H), 4.22 (s, 2H), 3.78 (s, 2H), 3.74–3.61 (m, 2H), 3.44 (d, ^2J(H,H) = 11.7 Hz, 1H), 3.24–3.14 (m, 1H), 2.51–2.46 (m, 1H), 2.42–2.35 (m, 1H), 2.29 ppm (d, ^2J(H,H) = 15.6 Hz, 1H); ^{13}C NMR ([D$_6$]DMSO): δ = 171.1, 164.0, 150.2, 141.4, 136.0, 134.8, 130.7, 126.9, 124.0, 123.7, 121.0, 120.1, 118.4, 118.3, 111.4, 106.6, 67.1, 66.9, 49.3, 42.5, 33.0, 30.6, 30.1 ppm; MS (ES+) *m/z* (%): 464 (100) $[M+H]^+$; HRMS (ES+) *m/z* calcd for $C_{25}H_{26}N_3O_6$: 464.182161, found: 464.185742; Anal. calcd for $C_{25}H_{26}N_3O_6Cl\cdot1H_2O$: C 57.97, H 5.45, N 8.11, found: C 58.31, H 5.28, N 8.03.

(*R*,*S*)-5-(Naphthalene-1-carbonyloxymethyl)-3-(4-nitrobenzoyloxymethyl)-2,3,4,7-tetrahydro-1*H*-azepine hydrochloride [(*rac*)-7]: Use of (*rac*)-**21** (0.129 g, 0.230 mmol) gave 0.104 g (91%) of (*rac*)-**7** as colorless solid: mp: 115 °C; ^{1}H NMR ([D$_6$]DMSO): δ = 9.47 (bs, 1H), 9.15 (bs, 1H), 8.74 (d, ^3J(H,H) = 8.5 Hz, 1H), 8.20–8.14 (m, 4H), 8.10 (d, ^3J(H,H) = 8.7 Hz, 2H), 8.01 (d, ^3J(H,H) = 8.0 Hz, 1H), 7.64 (t, ^3J(H,H) = 7.3 Hz, 1H), 7.61–7.55 (m, 2H), 6.01 (t, ^3J(H,H) = 5.4 Hz, 1H), 4.92 (d, ^2J(H,H) = 13.1 Hz, 1H), 4.87 (d, ^2J(H,H) = 13.3 Hz, 1H), 4.36 (dd, ^2J(H,H) = 11.0, ^3J(H,H) = 6.0 Hz, 1H), 4.30 (dd, ^2J(H,H) = 11.0, ^3J(H,H) = 6.4 Hz, 1H), 3.86–3.71 (m, 2H), 3.56–3.48 (m, 1H), 3.31–3.20 (m, 1H), 2.66 (dd, ^2J(H,H) = 15.6, ^3J(H,H) = 11.0 Hz, 1H), 2.56 (d, ^2J(H,H) = 15.4 Hz, 1H), 2.54–2.46 ppm (m, 1H); ^{13}C NMR ([D$_6$]DMSO): δ = 166.4, 164.1, 150.2, 141.6, 134.8, 133.7, 133.5, 130.6, 130.5, 130.1, 128.8, 128.1, 126.5, 126.3, 125.1, 124.9, 123.7, 121.6, 68.4, 66.9, 49.7, 42.9, 33.5, 30.5 ppm; MS (ES+) *m/z* (%): 461 (100) $[M+H]^+$; HRMS (ES+) *m/z* calcd for $C_{26}H_{25}N_2O_6$: 461.171262, found: 461.174019; Anal. calcd for $C_{26}H_{25}N_2O_6Cl\cdot1H_2O$: C 60.64, H 5.29, N 5.44, found: C 60.70, H 5.47, N 5.35.

(*R*,*S*)-3-Benzoyloxymethyl-5-(4-nitrobenzoyloxymethyl)-2,3,4,7-tetrahydro-1*H*-azepine hydrochloride [(*rac*)-8]: Use of (*rac*)-**23** (0.123 g, 0.240 mmol) yielded 0.094 g (88%) of (*rac*)-**8** as colorless powder: mp: 206 °C; ^{1}H NMR ([D$_6$]DMSO): δ = 9.44 (bs, 1H), 9.13 (bs, 1H), 8.31 (d, ^3J(H,H) = 8.7 Hz, 2H), 8.19 (d, ^3J(H,H) = 8.7 Hz, 2H), 7.97 (d, ^3J(H,H) = 7.3 Hz, 2H), 7.65 (t, ^3J(H,H) = 7.3 Hz, 1H), 7.50 (t, ^3J(H,H) = 7.7 Hz, 2H), 5.97 (t, ^3J(H,H) = 5.4 Hz, 1H), 4.87 (d, ^2J(H,H) = 14.7 Hz, 1H), 4.84 (d, ^2J(H,H) = 14.0 Hz, 1H), 4.27 (d, ^3J(H,H) = 6.0 Hz, 2H), 3.85–3.69 (m, 2H), 3.50 (d, ^2J(H,H) = 12.1 Hz, 1H), 3.29–3.18 (m, 1H), 2.62 (dd, ^2J(H,H) = 15.6, ^3J(H,H) = 10.6 Hz, 1H), 2.49 (d, ^2J(H,H) = 14.7 Hz, 1H), 2.49–2.44 ppm (bs, 1H); ^{13}C NMR ([D$_6$]DMSO): δ = 165.4, 163.7, 150.2, 140.8, 134.7, 133.3, 130.5, 129.3, 129.0, 128.6, 123.7, 121.4, 68.7, 66.0, 49.4, 42.6, 33.3, 30.3 ppm; MS (ES+) *m/z* (%): 411 (100) $[M+H]^+$; HRMS (ES+) *m/z* calcd for $C_{22}H_{23}N_2O_6$: 411.155612, found: 411.153340; Anal. calcd for $C_{22}H_{23}N_2O_6Cl\cdot1/2H_2O$: C 57.96, H 5.13, N 6.41, found: C 58.18, H 5.41, N 5.71.

(*R*,*S*)-5-(4-Bromobenzoyloxymethyl)-3-(4-nitrobenzoyloxymethyl)-2,3,4,7-tetrahydro-1*H*-azepine hydrochloride [(*rac*)-12]: According to the general procedure, employment of (*rac*)-**22** (0.071 g, 0.120 mmol) rendered 0.059 g (94%) of (*rac*)-**12** as a colorless solid: mp: 194 °C; ^{1}H NMR ([D$_4$]MeOH): δ = 8.27 (d, ^3J(H,H) = 8.9 Hz, 2H), 8.19 (d, ^3J(H,H) = 8.9 Hz, 2H), 7.89 (d, ^3J(H,H) = 8.7 Hz, 2H), 7.60 (d, ^3J(H,H) = 8.7 Hz, 2H), 6.04 (t, ^3J(H,H) = 5.7 Hz, 1H), 4.88 (d, ^2J(H,H) = 13.5 Hz, 1H), 4.82 (d, ^2J(H,H) = 13.1 Hz, 1H), 4.40 (dd, ^2J(H,H) = 11.2, ^3J(H,H) = 6.2 Hz, 1H), 4.36 (dd, ^2J(H,H) = 11.2, ^3J(H,H) = 6.4 Hz,1H), 3.91 (dd, ^2J(H,H) = 15.3, ^3J(H,H) = 6.1 Hz, 1H), 3.86 (dd, ^2J(H,H) = 15.4, ^3J(H,H) = 5.8 Hz, 1H), 3.68 (dd, ^2J(H,H) = 13.2, ^3J(H,H) = 3.4 Hz, 1H), 3.36 (dd, ^2J(H,H) = 13.1, ^3J(H,H) = 10.5 Hz, 1H), 2.71–2.61 (m, 2H), 2.60–2.51 ppm (m, 1H); ^{13}C NMR ([D$_6$]DMSO): δ = 164.8, 164.2, 150.4, 141.3, 134.9, 132.0, 131.2, 130.8, 128.7, 127.7, 123.8, 121.3, 68.4, 67.0, 49.6, 42.8, 33.4, 30.4 ppm; MS (ES+) *m/z* (%): 489 (100) $[M+H]^+$; HRMS (ES+) *m/z* calcd for $C_{22}H_{22}N_2O_6Br$: 489.066123, found: 489.065860; Anal. calcd for $C_{22}H_{22}BrClN_2O_6$: C 50.26, H 4.22, N 5.33, found: C 50.21, H 4.53, N 5.22.

(*R*,*S*)-3,5-Bis-(4-nitrobenzoyloxymethyl)-2,3,4,7-tetrahydroazepine-1-carboxylic acid *tert*-butyl ester [(*rac*)-25]: *p*-Nitrobenzoic acid (0.485 g, 2.90 mmol, 2.4 equiv) and DMAP (5 mol%) were added to a stirred solution of (*rac*)-**24** (0.295 g, 1.2 mmol, 1.0 equiv) in a 1:1 mixture of THF and CH_2Cl_2, followed by the addition of a solution of DIC (1.3 equiv) in the above solvent mixture. The reaction mixture was stirred at room temperature for 13 h and then carefully quenched by the addition of a saturated $NaHCO_3$ solution. After addition of Et_2O, the layers were separated. The organ-

ic layer was filtered, and the residue was washed three times with Et_2O. The combined filtrates were washed twice with brine, dried over $MgSO_4$, filtered, and concentrated under reduced pressure. Column chromatography (hexanes/*t*BuOMe: 1:1) of the oily residue afforded 0.461 g (69%) of (*rac*)-**25** as a colorless solid: mp: 124 °C; ^{1}H NMR (rotamers ~1:1): δ = 8.26 (d, ^3J(H,H) = 7.6 Hz, 4H), 8.21–8.14 (m, 4H), 5.99–5.90 (bd, 1H), 4.80 (d, ^2J(H,H) = 12.6 Hz, 1H), 4.75 (d, ^2J(H,H) = 12.6 Hz, 1H), 4.40–4.26 (m, 2H), 4.16–3.96 (m, 2H), 3.75–3.66 (m, 1H), 3.63–3.48 (m, 1H), 2.60–2.41 (m, 2H), 2.33 (dd, ^2J(H,H) = 15.5, ^3J(H,H) = 8.5 Hz, 1H), 1.46 ppm (s, 9H); ^{13}C NMR (rotamers): δ = 164.4, 164.3, 155.3, 155.0, 150.5, 135.2, 135.1, 134.8, 133.9, 130.6, 130.5, 128.4, 128.2, 123.50, 123.46, 80.2, 79.9, 70.5, 70.4, 67.4, 49.1, 48.9, 46.4, 46.3, 36.9, 36.6, 29.8, 29.5, 28.32, 28.27 ppm; MS (ES+) *m/z* (%): 578 (100) $[M+Na]^+$, 1133 (51) $[2M+Na]^+$; HRMS (ES+) *m/z* calcd for $C_{27}H_{29}N_3O_{10}Na$: 578.175064, found: 578.175497; Anal. calcd for $C_{27}H_{29}N_3O_{10}$: C 57.39, H 5.30, N 7.44, found: C 57.34, H 5.22, N 7.22.

(*R*,*S*)-3,5-Bis-(4-aminobenzoyloxymethyl)-2,3,4,7-tetrahydro-1*H*-azepine trihydrochloride [(*rac*)-**11**]**:** According to the general procedure, employment of (*rac*)-**25** (0.230 g, 0.4 mmol, 1.0 equiv) provided 0.119 g (59%) of (*rac*)-**11** as a brownish solid: mp: >250 °C; ^{1}H NMR ([D$_6$]DMSO): δ = 9.67 (bs, 1H), 9.27 (bs, 1H), 7.74 (bs, 4H), 7.40–6.90 (bs, 6H), 6.81 (bs, 4H), 5.86 (s, 1H), 4.68 (s, 2H), 4.15 (s, 2H), 3.82–3.60 (m, 2H), 3.41 (bs, 1H), 3.16 (bs, 1H), 3.03 (s, 1H), 2.40–2.32 ppm (m, 2H); ^{13}C NMR ([D$_6$]DMSO): δ = 165.3, 165.0, 149.5, 141.8, 130.9, 119.9, 118.3, 115.3, 66.9, 65.3, 49.5, 42.5, 33.3, 30.4 ppm; MS (ES+) *m/z* (%): 396 (100) $[M+H]^+$, 791 (14) $[2M+H]^+$; HRMS (ES+) *m/z* calcd for $C_{22}H_{26}N_3O_4$: 396.192332, found: 396.195761; Anal. calcd for $C_{22}H_{28}N_3O_4Cl_3\cdot 2H_2O$: C 48.85, H 5.96, N 7.77, found: C 48.43, H 5.84, N 7.63.

(*R*,*S*)-3,5-Bis-(4-nitrobenzoyloxymethyl)-2,3,4,7-tetrahydro-1*H*-azepine hydrochloride [(*rac*)-**10**]**:** According to the general procedure, employment of (*rac*)-**25** (0.117 g, 0.210 mmol) furnished 0.099 g (96%) of (*rac*)-**10** as a colorless solid: mp: 104 °C; ^{1}H NMR ([D$_6$]DMSO): δ = 9.57 (bs, 1H), 9.23 (bs, 1H), 8.29 (d, ^3J(H,H) = 8.7 Hz, 2H), 8.28 (d, ^3J(H,H) = 8.7 Hz, 2H), 8.19 (d, ^3J(H,H) = 8.9 Hz, 2H), 8.18 (d, ^3J(H,H) = 8.7 Hz, 2H), 5.97 (t, ^3J(H,H) = 5.5 Hz, 1H), 4.87 (d, ^2J(H,H) = 13.3 Hz, 1H), 4.82 (d, ^2J(H,H) = 13.3 Hz, 1H), 4.35 (d, ^2J(H,H) = 12.8 Hz, 1H), 4.31 (d, ^2J(H,H) = 12.6 Hz, 1H), 3.80 (dd, ^2J(H,H) = 15.2, ^3J(H,H) = 5.6 Hz, 1H), 3.74 (dd, ^2J(H,H) = 15.2, ^3J(H,H) = 5.6 Hz, 1H), 3.50 (d, ^2J(H,H) = 10.5 Hz, 1H), 3.29–3.22 (m, 1H), 2.63 (dd, ^2J(H,H) = 15.8, ^3J(H,H) = 10.2 Hz, 1H), 2.57–2.53 ppm (m, 2H); ^{13}C NMR ([D$_6$]DMSO): δ = 164.0, 163.8, 150.19, 150.18, 140.9, 134.8, 134.7, 130.63, 130.59, 123.8, 123.7, 121.5, 68.7, 66.8, 49.4, 42.6, 33.3, 30.2 ppm; MS (ES+) *m/z* (%): 456 (100) $[M+H]^+$; HRMS (ES+) *m/z* calcd for $C_{22}H_{22}N_3O_8$: 456.140690, found: 456.143014; Anal. calcd for $C_{22}H_{22}N_3O_8Cl\cdot 1H_2O$: C 51.82, H 4.74, N 8.24, found: C 51.70, H 4.72, N 8.14.

Acknowledgements

We gratefully acknowledge the financial support of our research by the DFG-Graduiertenkolleg GRK 541 "Proteinfunktion auf atomarer Ebene" (T.L.) and the DPhG within the fellowship "DPhG-Stiftung zur Förderung des wissenschaftlichen Nachwuchses" (W.E.D.). The authors are grateful to J. Böttcher for constructive discussions. The clone of the protease was kindly provided by Prof. Dr. Daniel E. Goldberg, Department of Molecular Microbiology, Washington University School of Medicine, St. Louis, MO (USA).

Keywords: combinatorial docking · inhibitor design · malaria · molecular dynamics · plasmepsin

[1] WHO, The World Health Report **2004**.
[2] S. E. Francis, I. Y. Gluzman, A. Oksman, A. Knickerbocker, R. Mueller, M. L. Bryant, D. R. Sherman, D. G. Russell, D. E. Goldberg, *EMBO J.* **1994**, *13*, 306–317.
[3] D. E. Goldberg, A. F. G. Slater, R. Beavis, B. Chait, A. Cerami, G. B. Henderson, *J. Exp. Med.* **1991**, *173*, 961–969.
[4] I. Y. Gluzman, S. E. Francis, A. Oksman, C. E. Smith, K. L. Duffin, D. E. Goldberg, *J. Clin. Invest.* **1994**, *93*, 1602–1608.
[5] J. B. Dame, G. R. Reddy, C. A. Yowell, B. M. Dunn, J. Kay, C. Berry, *Mol. Biochem. Parasitol.* **1994**, *64*, 177–190.
[6] M. J. Humphreys, R. P. Moon, A. Klinder, S. D. Fowler, K. Rupp, D. Bur, R. G. Ridley, C. Berry, *FEBS Lett.* **1999**, *463*, 43–48.
[7] R. Banerjee, J. Liu, W. Beatty, L. Pelosof, M. Klemba, D. E. Goldberg, *Proc. Natl. Acad. Sci. USA* **2002**, *99*, 990–995.
[8] F. Salas, J. Fichmann, G. K. Lee, M. D. Scott, P. J. Rosenthal, *Infect. Immun.* **1995**, *63*, 2120–2125.
[9] P. S. Sijwali, K. Kato, K. B. Seydel, J. Gut, J. Lehman, M. Klemba, D. E. Goldberg, L. H. Miller, P. J. Rosenthal, *Proc. Natl. Acad. Sci. USA* **2004**, *101*, 8721–8726.
[10] B. R. Shenai, P. S. Sijwali, A. Singh, P. J. Rosenthal, *J. Biol. Chem.* **2000**, *275*, 29000–29010.
[11] P. S. Sijwali, P. J. Rosenthal, *Proc. Natl. Acad. Sci. USA* **2004**, *101*, 4384–4389.
[12] P. S. Sijwali, B. R. Shenai, J. Gut, A. Singh, P. J. Rosenthal, *Biochem. J.* **2001**, *360*, 481–489.
[13] K. K. Eggleson, K. L. Duffin, D. E. Goldberg, *J. Biol. Chem.* **1999**, *274*, 32411–32417.
[14] M. Klemba, I. Gluzman, D. E. Goldberg, *J. Biol. Chem.* **2004**, *279*, 43000–43007.
[15] G. H. Coombs, D. E. Goldberg, M. Klemba, C. Berry, J. Kay, J. C. Mottram, *Trends Parasitol.* **2001**, *17*, 532–537.
[16] R. P. Moon, L. Tyas, U. Certa, K. Rupp, D. Bur, C. Jacquet, H. Matile, H. Loetscher, F. Grueninger-Leitch, J. Kay, B. M. Dunn, C. Berry, R. G. Ridley, *Eur. J. Biochem.* **1997**, *244*, 552–560.
[17] C. Boss, S. Richard-Bildstein, T. Weller, W. Fischli, S. Meyer, C. Binkert, *Curr. Med. Chem.* **2003**, *10*, 883–907.
[18] C. Boss, O. Corminboeuf, C. Grisostomi, S. Meyer, A. F. Jones, L. Prade, C. Binkert, W. Fischli, T. Weller, D. Bur, *ChemMedChem* **2006**, *1*, 1341–1345.
[19] A. L. Omara-Opyene, P. A. Moura, C. R. Sulsona, J. A. Bonilla, C. A. Yowell, H. Fujioka, D. A. Fidock, J. B. Dame, *J. Biol. Chem.* **2004**, *279*, 54088–54096.
[20] J. Liu, I. Y. Gluzman, M. E. Drew, D. E. Goldberg, *J. Biol. Chem.* **2005**, *280*, 1432–1437.
[21] J. Liu, E. S. Istvan, I. Y. Gluzman, J. Gross, D. E. Goldberg, *Proc. Natl. Acad. Sci. USA* **2006**, *103*, 8840–8845.
[22] J. A. Bonilla, T. D. Bonilla, C. A. Yowell, H. Fujioka, J. B. Dame, *Mol. Microbiol.* **2007**, *65*, 64–75.
[23] J. B. Dame, C. A. Yowell, L. Omara-Opyene, J. M. Carlton, R. A. Cooper, T. Li, *Mol. Biochem. Parasitol.* **2003**, *130*, 1–12.
[24] K. Ersmark, B. Samuelsson, A. Hallberg, *Med. Res. Rev.* **2006**, *26*, 626–666.
[25] C. Oefner, A. Binggeli, V. Breu, D. Bur, J. P. Clozel, A. D'Arcy, A. Dorn, W. Fischli, F. Grüninger, R. Güller, G. Hirth, H. P. Märki, S. Mathews, M. Müller, R. G. Ridley, H. Stadler, E. Vieira, M. Wilhelm, F. K. Winkler, W. Wostl, *Chem. Biol.* **1999**, *6*, 127–131.
[26] E. Specker, J. Böttcher, H. Lilie, A. Heine, A. Schoop, G. Müller, N. Griebenow, G. Klebe, *Angew. Chem.* **2005**, *117*, 3200–3204; *Angew. Chem. Int. Ed.* **2005**, *44*, 3140–3144.
[27] D. A. Carcache, S. R. Hörtner, A. Bertogg, C. Binkert, D. Bur, H. P. Märki, A. Dorn, F. Diederich, *ChemBioChem* **2002**, *3*, 1137–1141.
[28] F. Hof, A. Schütz, C. Fäh, S. Meyer, D. Bur, J. Liu, D. E. Goldberg, F. Diederich, *Angew. Chem.* **2006**, *118*, 2193–2196; *Angew. Chem. Int. Ed.* **2006**, *45*, 2138–2141.
[29] A. M. Silva, A. Y. Lee, S. V. Gulnik, P. Majer, J. Collins, T. N. Bhat, P. J. Collins, R. E. Cachau, K. E. Luker, I. Y. Gluzman, S. E. Francis, A. Oksman, D. E. Goldberg, J. W. Erickson, *Proc. Natl. Acad. Sci. USA* **1996**, *93*, 10034–10039.

[30] O. A. Asojo, E. Afonina, S. V. Gulnik, B. Yu, J. W. Erickson, R. Randad, D. Medjahed, A. M. Silva, *Acta Crystallogr. Sect D: Biol. Crystallogr.* **2002**, *58*, 2001–2008.
[31] O. A. Asojo, S. V. Gulnik, E. Afonina, B. Yu, J. A. Ellman, T. S. Haque, A. M. Silva, *J. Mol. Biol.* **2003**, *327*, 173–181.
[32] L. Prade, A. F. Jones, C. Boss, S. Richard-Bildstein, S. Meyer, C. Binkert, D. Bur, *J. Biol. Chem.* **2005**, *280*, 23837–23843.
[33] K. Ersmark, I. Feierberg, S. Bjelic, E. Hamelink, F. Hackett, M. J. Blackman, J. Hultén, B. Samuelsson, J. Åqvist, A. Hallberg, *J. Med. Chem.* **2004**, *47*, 110–122.
[34] K. Ersmark, I. Feierberg, S. Bjelic, J. Hultén, B. Samuelsson, J. Åqvist, A. Hallberg, *Bioorg. Med. Chem.* **2003**, *11*, 3723–3733.
[35] S. Weik, T. Luksch, A. Evers, J. Böttcher, C. A. Sotriffer, A. Hasilik, H.-G. Löffler, G. Klebe, J. Rademann, *ChemMedChem* **2006**, *1*, 445–457.
[36] K. Ersmark, M. Nervall, E. Hamelink, L. K. Janka, J. C. Clemente, B. M. Dunn, M. J. Blackman, B. Samuelsson, J. Åqvist, A. Hallberg, *J. Med. Chem.* **2005**, *48*, 6090–6106.
[37] M. G. Bursavich, D. H. Rich, *J. Med. Chem.* **2002**, *45*, 541–558.
[38] D. A. Carcache, S. R. Hörtner, P. Seiler, F. Diederich, A. Dorn, H. P. Märki, C. Binkert, D. Bur, *Helv. Chim. Acta* **2003**, *86*, 2173–2191.
[39] S. Brass, N.-S. Chan, C. Gerlach, T. Luksch, J. Böttcher, W. E. Diederich, *J. Organomet. Chem.* **2006**, *691*, 5406–5422.
[40] M. Rarey, T. Lengauer, *Perspect. Drug Discovery Des.* **2000**, *20*, 63–81.
[41] J. Sadowski, J. Gasteiger, G. Klebe, *J. Chem. Inf. Comput. Sci.* **1994**, *34*, 1000–1008.
[42] R. Pedrosa, C. Andrés, A. Gutiérrez-Loriente, J. Nieto, *Eur. J. Org. Chem.* **2005**, *12*, 2449–2458.
[43] F. H. Allen, *Acta Crystallogr. Sect. B: Struct. Sci* **2002**, *58*, 380–388.
[44] S. Kabuß, H. G. Schmid, H. Friebolin, W. Faißt, *Org. Magn. Reson.* **1969**, *1*, 451–465.
[45] E. Grunwald, E. Price, *J. Am. Chem. Soc.* **1965**, *87*, 3139–3147.
[46] H. Gutiérrez-de-Terán, M. Nervall, K. Ersmark, P. Liu, L. K. Janka, B. Dunn, A. Hallberg, J. Åqvist, *Biochemistry* **2006**, *45*, 10529–10541.
[47] S. Schmitt, D. Kuhn, G. Klebe, *J. Mol. Biol.* **2002**, *323*, 387–406.
[48] D. Kuhn, N. Weskamp, S. Schmitt, E. Hüllermeier, G. Klebe, *J. Mol. Biol.* **2006**, *359*, 1023–1044.
[49] P. R. Gerber, K. Müller, *J. Comput. Aided Mol. Des.* **1995**, *9*, 251–268.
[50] Chemical Computing Group, Molecular Operating Environment (MOE), 2006.08, Montréal, QC (Canada) **2006**.
[51] S. Henikoff, J. G. Henikoff, *Proc. Natl. Acad. Sci. USA* **1992**, *89*, 10915–10919.
[52] D. A. Case, T. E. Cheatham, T. Darden, H. Gohlke, R. Luo, K. M. Merz, A. Onufriev, C. Simmerling, B. Wang, R. J. Woods, *J. Comput. Chem.* **2005**, *26*, 1668–1688.
[53] W. L. Jorgensen, J. Chandrasekhar, J. D. Madura, R. W. Impey, M. L. Klein, *J. Chem. Phys.* **1983**, *79*, 926–935.
[54] T. Darden, D. York, L. Pedersen, *J. Chem. Phys.* **1993**, *98*, 10089–10092.
[55] W. Humphrey, A. Dalke, K. Schulten, *J. Mol. Graph.* **1996**, *14*, 33–38.
[56] M. Rarey, B. Kramer, T. Lengauer, G. Klebe, *J. Mol. Biol.* **1996**, *261*, 470–489.
[57] Tripos Inc., Sybyl, St. Louis, MO (USA) **2004**.
[58] M. Hendlich, A. Bergner, J. Günther, G. Klebe, *J. Mol. Biol.* **2003**, *326*, 607–620.
[59] W. L. DeLano, *The PyMol Molecular Graphics System*, DeLano Scientific, San Carlos, CA (USA) **2002**, http://pymol.sourceforge.net/ (last access July 17, 2008).

Received: September 26, 2007
Revised: June 29, 2008
Published online on August 27, 2008

